

10204  
NACA TN 3838

0066760

TECH LIBRARY KAFB, NM

# NATIONAL ADVISORY COMMITTEE FOR AERONAUTICS

TECHNICAL NOTE 3838

PERFORMANCE CHARACTERISTICS OF RING-CASCADE-TYPE  
THRUST REVERSERS

By Jack G. McArdle

Lewis Flight Propulsion Laboratory  
Cleveland, Ohio



Washington  
November 1956

AFM C  
TECHNICAL STAFF  
AFL 2811



## TECHNICAL NOTE 3838

## PERFORMANCE CHARACTERISTICS OF RING-CASCADE-TYPE THRUST REVERSERS

By Jack G. McArdle

## SUMMARY

Model ring-cascade thrust reversers were tested in quiescent air to determine the effect of geometric design variables on performance and reversed-flow fields. The configurations consisted of a cascade of turning rings plus a mechanical deflector positioned aft of a 4-inch exhaust nozzle with a  $7^\circ$  external fairing. Reverse-thrust ratios up to 68 percent were obtained. The most important variables affecting performance were found to be deflector blockage, reverser working area, and ring spacing ratio. When the reversed-flow field was altered to obtain a two-lobed pattern by any of the several methods tested, the reverse-thrust ratio was reduced. The modulation characteristics of a typical shrouded ring-cascade reverser were found to be satisfactory.

## INTRODUCTION

Many methods have been proposed for reducing the ground roll of modern high-speed jet aircraft. One method which appears to offer promise is the thrust reverser, which reverses the direction of engine thrust to provide a braking force. Results of an analysis (ref. 1) indicated that conventional wheel brakes plus reverse thrust in the order of 40 percent of the maximum forward thrust would be sufficient to stop an airplane on an icy runway in the same distance it could be stopped with brakes alone on a dry runway.

In addition to ground-roll reduction, the modulating characteristics of thrust reversers also make them suitable as a means of regulating engine net thrust over the whole forward and reverse range while maintaining full engine speed. Thus, these devices also appear attractive as a means of controlling aircraft landing approach and dive velocity.

A research program using scale models was conducted at the NACA Lewis laboratory to determine design criteria for practical thrust-reverser devices. The purpose of the program was to examine several

basic types of reversers and to determine their performance and operating characteristics. The results of investigations of hemispherical target, cylindrical target, and tailpipe-cascade types of reversers are reported in references 2 to 5. The present report describes the various geometric factors which affect the performance and reversed-flow fields of scale-model ring-cascade reversers, which, when in operation, consist of a set of turning rings positioned behind the exhaust nozzle. The exhaust jet is deflected into the rings by a mechanical obstruction called a deflector, placed in the center of the jet downstream of the exhaust-nozzle exit. Unlike the tailpipe-cascade reverser, the ring-cascade reverser can be made completely separate from the engine and tailpipe.

The significant geometric factors and the range of variables tested are ring spacing ratios from 0.095 to 0.28, number of rings from 2 to 10, round and rectangular deflectors having blockages up to 50 percent of the exhaust-nozzle area, and shrouds over the rings blocking up to 50 percent of the flow area. The tests were conducted over a range of exhaust-nozzle pressure ratios up to 2.5. For some of the configurations, the reversed-flow fields and the thrust-modulation performance were obtained.

All tests were made in quiescent ambient air using unheated flow and a 4-inch exhaust nozzle with  $7^\circ$  external fairing.

## PRINCIPLES AND GEOMETRIC FACTORS

### Principles

The principles of operation of a ring-cascade thrust reverser using a mechanical deflector are illustrated in the schematic sketch of figure 1. The essential parts of the reversing mechanism are the deflector and the cascade of turning rings. Gas from the exhaust nozzle is directed toward the cascade by the deflector. The gas which enters the cascade is further turned by the rings and produces reverse thrust, while the gas which escapes rearward (if any) produces forward thrust. If the reversed flow attaches to or impinges on the fairing, additional thrust, either reverse or forward, will be produced by the pressures acting on the fairing. The resultant thrust is the vector sum of the axial components of all forces acting on the model.

A brief discussion of the geometric factors involved in the operation of a ring-cascade reverser and the manner in which they may be expected to influence performance is presented in the following paragraphs. The symbols used in this report are defined in appendix A.

## Deflector

Deflector blockage. - Deflector blockage is defined as  $A_d/A_n$  where  $A_d$  is the projected area of the deflector and  $A_n$  is the exhaust-nozzle-exit area. Increasing deflector blockage may be expected to increase reverse-thrust ratio because for constant cascade geometry larger deflectors should deflect a larger portion of the jet into the cascade.

Deflector shape. - The shape of the deflector may be expected to affect the manner in which the jet is apportioned to the cascade. Two extremes in deflector shape, the disk and the long rectangle, were tested.

Deflector spacing ratio. - Deflector spacing ratio is defined as  $x/D_n$ , where  $x$  is the axial distance from the nozzle exit to the deflector (as shown in figs. 1 and 2) and  $D_n$  is the exhaust-nozzle-exit diameter. Reducing the deflector spacing ratio may be expected to increase the reverse-thrust ratio by causing a larger portion of the jet to enter the cascade. However, a minimum deflector spacing ratio should exist such that further reductions in deflector spacing will cause reduction of the nozzle air flow because of the stagnant region ahead of the deflector. This spacing is defined as the minimum deflector spacing ratio for 100-percent air flow ratio. Air flow ratio is defined in appendix B.

## Cascade

Ring cross-sectional design. - Two ring-inlet angles were investigated because it was expected that the angle of attack at the cascade entrance would affect the performance and length of the cascade. The rings tested (fig. 3) had an inside diameter slightly larger than the exhaust-nozzle diameter so that the rings would fit over the nozzle.

Ring spacing ratio. - Ring spacing ratio is defined as  $S/D_n$ , where  $S$  is the axial distance between corresponding points on adjacent rings. This parameter may be expected to affect reverse-thrust ratio because it is a measure of the cascade solidity for a given ring design. For simplicity, only cascades having constant ring spacing ratio throughout the cascade were tested.

First-ring spacing ratio. - First-ring spacing ratio  $l/D_n$ , where  $l$  is the axial distance between the leading edge of the first ring and the exhaust-nozzle exit, may be expected to affect reverse-thrust ratio for the same reason as the deflector spacing ratio. In addition, the first-ring spacing ratio should have a large influence on the over-all length of the reverser.

Reverser area. - By Newton's Second Law of Motion it can be shown that the reverse thrust produced by any reverser is

$$\int p \, dA = F_{j,n}$$

where  $A$  represents the total projected area of the reverser and  $p$  is the pressure difference acting across an element of area. For the ring-cascade reverser, the total projected area will be called the working area and is defined as  $NA_r + A_d$ .

The pressure available to produce reverse thrust is limited by the nozzle pressure ratio, but the working area can be significantly changed by varying the number or size of the rings in the cascade. However, increasing the working area above the minimum required to handle the deflected jet will have little or no effect on performance.

Shrouding. - In some installations it might be necessary to alter the reversed-flow field to prevent the exhaust from striking critical parts of the aircraft structure. If the reversed-flow field is altered by shrouds placed on portions of the cascade, the reverse-thrust ratio will probably decrease because the shrouds will force some of the jet to exhaust to the rear. The magnitude of the decrease will depend upon the deflector shape and the amount of shrouding.

## APPARATUS AND INSTRUMENTATION

### Apparatus

The model ring-cascade reversers tested during this investigation consisted of a cascade of turning rings plus a mechanical deflector positioned aft of an exhaust nozzle with a  $7^\circ$  external fairing. This apparatus, together with some of the pertinent dimensions, is shown schematically in figure 4; and a photograph of a typical reverser is shown in figure 5. A summary of configurations tested is given in table I.

Deflector designs. - The deflector designs which were tested are shown in figure 2. All deflectors were mounted on a rod which ran along the axis of the cascade and, in turn, was secured to four mounting rods extending from the fairing.

Ring designs. - The ring cross-sectional designs used in this investigation are shown in figure 3. Figure 6 is a photograph of a typical ring and shows the arms used to position the rings on the four mounting rods. The rings were held in cascade by means of spacers between arms of adjacent rings.

Modifications to alter reversed-flow boundaries. - Internal and external portions of the cascade on some of the configurations were shrouded to change the shape of the reversed-flow field. A photograph of a shrouded ring-cascade reverser is shown in figure 7. The shrouds were, in all cases, secured directly to the rings.

Model used to determine modulation characteristics. - The modulation characteristics of a shrouded ring-cascade reverser were determined with an adjustable model in which the deflector position was varied by interconnected electric actuators. The deflector position was read by a calibrated electric indicator. A rear-view photograph of this configuration with the deflector in maximum-blockage position is shown in figure 8.

Experimental setup. - The experimental setup upon which all tests were conducted is shown in figure 9. The air-supply duct was connected to the laboratory air system by flexible bellows and pivoted to a steel frame so that axial-thrust forces along the pipe, both forward and reverse, could be freely transmitted to and directly read from a balanced-pressure-diaphragm, null-type, thrust-measuring cell. In order to ensure that the steel strap used to transmit the force from the duct to the thrust cell was always in tension, it was sometimes necessary to preload the system with counterweights. A blast deflector, which was attached to the floor of the test cell, was placed around the fairing to prevent the reversed flow from impinging on the air-supply-duct flanges.

### Instrumentation

Air flow through the system was measured by means of a standard A.S.M.E. sharp-edged orifice. Two total-pressure tubes, about 8 inches ahead of the exhaust-nozzle exit, were used to measure exhaust-nozzle total pressure, while a barometer was used to measure ambient exhaust pressure. Total-pressure rakes were located at two stations along the fairing in order to determine reversed-flow boundaries. The station locations and areas surveyed by the rakes are given in figure 4, and the rakes at the station nearest the exhaust nozzle appear in the photograph of figure 5.

### PROCEDURE

Forward jet thrust of the nozzle was measured over a range of exhaust-nozzle total- to ambient-pressure ratios up to 2.5. The rings and deflector were then attached and the net reverse thrust measured after setting the pressure ratio at the desired values. The pressure ratio was regulated by variation of the inlet pressure. In the case of the model used to determine the modulation characteristics, the deflector was actuated while the pressure ratio was held constant at 2.0.

The ratio of the net reverse thrust of a given configuration at a given pressure ratio to the forward thrust of the nozzle alone at the same pressure ratio was thus obtained and defined as the reverse-thrust ratio. The ratio of the air flow passed during reverse-thrust operation to the air flow passed during forward-thrust operation at the same pressure ratio was similarly obtained and defined as the air flow ratio. Jet thrusts and air flows were corrected for changes in inlet pressure. For the entire investigation, unheated air was used.

The reversed-flow fields were drawn from plots of total pressure against position made for each of the reversed-flow rakes. For the cases in which the rakes did not extend to the reversed-flow boundary, the total-pressure data were supplemented with field sketches and measurements.

## RESULTS AND DISCUSSION

Several methods of deflecting the exhaust jet into the rings have been used successfully by various investigators. A method is described in reference 6 in which a swirl produced by vanes in the tailpipe deflects the gas into the rings by centrifugal force. Methods for diverting the gas are reported in reference 7 in which a divergent attachment surface after the nozzle is used in conjunction with either a mechanical deflector or an air blast normal to the exhaust jet.

The initial stages of the program reported herein consisted of an exploratory investigation of the effectiveness of the three methods described of deflecting the jet into the rings. A method utilizing a mechanical deflector, but without the divergent attachment surface, was considered the most promising and was selected for the study of the various geometric parameters on ring-cascade reverser performance.

As described in the Apparatus section, the configurations discussed herein consisted of an exhaust nozzle with a  $7^\circ$  fairing, a cascade of turning rings large enough to fit over the exhaust nozzle, and a mechanical deflector. (Although the boattail shape used in these tests would possibly not be used in a full-scale installation, the boattail shape has only a small effect on performance, as reported in ref. 2.) The effects on reverse-thrust ratio  $\eta_R$  of the geometric variables shown in figure 1 (x, l, and S) plus some additional variables are presented in the following sections. All data are shown for an exhaust-nozzle pressure ratio of 2.0 and an air flow ratio of 100 percent with the exhaust nozzle choked, except in the cases where pressure ratio or air flow ratio is one of the variables used to construct the plot.

### Effect of Nozzle Pressure Ratio on Performance

The effect of nozzle pressure ratio on reverse-thrust ratio is shown in figure 10 for three ring designs and values of deflector blockage of 16, 25, and 50 percent. In general, performance with a deflector blockage of 50 percent is relatively insensitive to nozzle pressure ratio. As blockage is decreased below 50 percent, sensitivity increases, with reverse-thrust ratio generally falling off as the pressure ratio is increased. For the highest blockage, peak performance occurs near  $P_n/P_0$  of 2.0, and values of reverse-thrust ratio as high as 68 percent are attained. These configurations are typical of the ones tested in the course of this investigation.

The sharp drop in reverse-thrust ratio at a nozzle pressure ratio of approximately 1.4 for the  $O^0$ -entry rings and 16-percent-blockage deflector (fig. 10(b)) was observed to occur with several configurations (not shown in fig. 10) at low nozzle pressure ratios. The drop was most often associated with low-blockage disk deflectors. Although not definitely established, it is believed that this reproducible phenomenon is attributable to ring stall, to a sudden shift in the flow past the deflector, or both. However, it is felt that this characteristic will probably not be encountered in practice, because it occurs at pressure ratios and with geometries which will normally not be used. Generally, the reverse-thrust ratio at a nozzle pressure ratio of 2.0 is representative of that obtained in the pressure-ratio range from 1.8 to 2.4, which is the range of current operating interest.

Each of the plots in figure 10 shows that reverse-thrust ratio is a direct function of deflector blockage. This effect will be examined in the next section.

### Effect of Deflector Geometry on Performance

Although the data presented in this section are shown for optimum ring geometry (as will be discussed in the section Effect of Cascade Geometry on Performance), the effects reported are of a general nature.

Deflector blockage. - The effect of deflector blockage on reverse-thrust ratio is shown in figure 11 for three ring designs and flat-disk and flat-bar deflectors (figs. 2(a) and (b)). All data were obtained at the minimum deflector spacing ratio for an air flow ratio of 100 percent. As deflector blockage is increased, reverse-thrust ratio increases very rapidly at first then tends to level off. With complete blockage at the rear of the cascade, the ring designs used produced 72-percent reverse-thrust ratio. The flatness of the curve at high values of deflector blockage indicates that large blockage is not necessary. Full forward thrust was not attained at zero blockage because of gas pickup by the



rings resulting from normal spreading of the jet after it has left the nozzle. Full forward thrust would be regained by retracting the rings.

In an attempt to improve the performance of low-blockage deflectors, the 16-percent-blockage flat-disk and flat-bar deflectors were replaced with vented deflectors of the same blockage (figs. 2(c) and (d)). An increase in reverse-thrust ratio of 5 to 8 percentage points was measured. It was not determined whether the improvement was due to more complete turning of the flow through the vent or to an increase in pressure just behind the deflector lip.

When the 25-percent-blockage flat-bar deflector was replaced with a wedge-bar deflector of equal blockage (fig. 2(e)), a decrease in reverse-thrust ratio of 4 percentage points was measured. This wedge bar was designed to simulate a deflector which could be retracted by folding along the long edge.

Deflector spacing ratio. - The effect of deflector spacing ratio on reverse-thrust ratio is shown in figure 12 for a 16-percent-blockage flat-disk deflector at nozzle pressure ratios of 2.0 and 2.5. Deflector spacing ratios to the left of the vertical line result in reduced air flow ratio. For each pressure ratio, maximum reverse-thrust ratio occurs at the minimum deflector spacing ratio required for 100-percent air flow ratio.

A plot of the minimum deflector spacing ratio for 100-percent air flow ratio against deflector blockage is given in figure 13. All deflectors tested followed this curve. As expected, the minimum deflector spacing ratio for 100-percent air flow ratio increases as deflector blockage increases and decreases slightly for pressure ratios greater than 2.0, as shown by the single point for a pressure ratio of 2.5.

The air flow ratio is a measure of the effective flow area of the reverser. Reduced effective reverser flow area (as signified by reduced air flow ratio) would result in a change in the operating point of the engine when the reverser is in use.

#### Effect of Cascade Geometry on Performance

The data presented in this section were obtained using the flat-disk and flat-bar deflectors fixed in position at the minimum deflector spacing ratio required for 100-percent air flow ratio at an exhaust-nozzle pressure ratio of 2.0. Changes in cascade geometry (for the geometries tested) did not affect the air flow ratio, probably because the inside diameter of the rings was greater than the nozzle diameter.

Ring cross-sectional design and ring spacing ratio. - The effect of ring spacing ratio on reverse-thrust ratio is shown in figure 14 for three ring cross-sectional designs and three values of deflector blockage. Drawings of the rings are shown in figure 3.

In general, a maximum reverse-thrust ratio (over 60 percent) occurs within the range of ring spacing ratios tested. Optimum ring spacing ratios are about 0.25, 0.15, and 0.11 for the  $0^\circ$ -entry,  $60^\circ$ -entry single-curvature, and  $60^\circ$ -entry double-curvature rings, respectively. The  $0^\circ$ -entry rings are not as sensitive to changes in ring spacing ratio as the other two designs. Although the optimum ring spacing ratio is different for each ring design, it is relatively constant for varying amounts of deflector blockage. Tests showed that the  $0^\circ$ -entry rings gave best performance with the bar deflectors, while the  $60^\circ$ -entry rings always gave best performance with the disk deflectors.

On the basis of the limited amount of data taken, the rather unconventional design of the  $0^\circ$ -entry rings was successful apparently because of the nearly axial flow direction at the inlet to the rear portion of the cascade. This flow condition is shown schematically in figure 1, which was drawn from surveys made inside the cascade with a tuft probe.

In figure 15, comparison on the basis of the data in figure 14 is made of the reverser lengths necessary to produce 50-percent reverse-thrust ratio. The shortest reversers make use of  $60^\circ$ -entry rings and high deflector blockage. Lengths vary from 1.0 nozzle diameter for a reverser having six  $60^\circ$ -entry single-curvature rings with 50-percent-blockage disk deflector to 1.36 nozzle diameters for a reverser having six  $0^\circ$ -entry rings with 25-percent-blockage bar deflector. Sufficient data are available in this report so that comparison of other configurations can be made.

First-ring spacing ratio. - The effect of first-ring spacing ratio on reverse-thrust ratio is shown in figure 16 for two ring cross-sectional designs and three deflectors. For these tests, the deflector was fixed in position at the minimum spacing ratio required for 100-percent air flow ratio.

Reverse-thrust ratio is relatively insensitive to first-ring spacing ratio over a considerable range (0.15 to 0.35) for a wide variation in deflector geometry. However, when the first-ring spacing ratio was increased so much that the leading edge of the first ring was aft of the deflector, forward thrust was obtained and the deflector vibrated severely.

Number of rings. - Figure 17 illustrates the effect of varying the number of rings in the cascade on reverse-thrust ratio. Data are shown for three ring designs, ring spacing ratios at or near optimum, and various amounts of deflector blockage.

For all configurations, as the number of rings is increased, the reverse-thrust ratio increases rapidly at first then tends to level off. More of the double-curvature rings are required to produce a given reverse-thrust ratio because they are of smaller frontal area than the single-curvature rings.

As shown by the data for the  $0^\circ$ -entry rings, if performance is reduced by decreasing deflector blockage, all or most of the reduction can be regained by increasing the number of rings.

Reverser working area. - In figure 18 the reverse-thrust ratio is shown as a function of reverser working-area ratio, which is defined as  $(NA_r + A_d)/A_n$ . These are the same data as plotted in figure 17. The performance of hemispherical target reversers (from ref. 2) is given for comparison.

Although different ring-cascade configurations having the same working-area ratio do not produce equivalent amounts of reverse thrust, the performance trends are similar. Generalization of the performance was not accomplished, probably because the pressure distribution on the working area was different for each reverser. The pressure distribution would be expected to be dependent on ring and cascade geometry. In addition, the deflector makes up a small but significant part of the working area, because nozzle stagnation pressure exists on the upstream surface of the deflector. (An example of the importance of the deflector is found in fig. 18. The curves show that, if reversers having  $0^\circ$ -entry rings, a ring spacing ratio of 0.25, and a constant working-area ratio of 5.0 were tested, increasing the bar deflector blockage from 24 to 48 percent would increase the reverse-thrust ratio from 43 to 56 percent.)

The curves for the ring reversers are similar in shape to the curve for the hemispherical target reversers. The difference in peak reverse-thrust ratio can be attributed either to greater total-pressure losses in the cascades or to a change in gas turning angle because of the difference in lip angles ( $180^\circ$  for the hemispheres and approx.  $160^\circ$  for the rings), or both. The difference in peak reverse-thrust ratio is not due to any gas exhausting rearward, for it was visually observed that all the gas was deflected into the rings when the ring cascades produced peak reverse thrust.

In general, the ring-cascade reversers require about twice as much working area to produce peak reverse thrust as do the hemispheres. Inasmuch as nozzle stagnation pressure exists over most of the hemisphere working area (frontal area, ref. 2), it thus follows that high pressures probably do not occur on a large portion of the ring area. Figure 18 also shows that the small  $60^\circ$ -entry double-curvature rings make more efficient use of the available ring working area than do the larger single-curvature rings.

Although ring-cascade reversers having geometries comparable with those tested during this investigation require more working area than hemispherical target reversers, it may be possible to build a ring-cascade reverser having an installed weight about the same as the installed weight of a hemispherical target reverser. In addition, it is felt that ring-cascade devices may have practical advantages over some other types of reversers in ease of actuation and adaptation to low-drag fairings.

Blade arrangement. - A conventional ring cascade was altered in an attempt to form a reverser in which the rings were immersed sufficiently in the jet to produce reverse thrust without the use of a deflector. It was desired to build the cascade in two halves that could be moved into the jet from each side of the exhaust nozzle. The design was accomplished by splitting conventional rings along a diameter, removing a portion of the ring on either side of the split, and welding the remaining segments of the ring together. An exploded view of the resulting "split" cascade is shown in figure 19. Results of the test are given in figure 20, in which reverse-thrust ratio is plotted against ring spacing ratio. Data are shown for several configurations both with and without the use of a deflector. The performance of a conventional ring-cascade reverser is given for reference.

All split-cascade configurations produce forward thrust unless a deflector is used. With a 24-percent-blockage bar deflector, the conventional cascade gives 10 percent greater reverse-thrust ratio than the split cascade. Thus, on the basis of performance, the split cascade offers no advantage; however, with a deflector, over 40-percent reverse-thrust ratio is possible.

#### Reversed-Flow Boundaries

The reversed-flow characteristics of typical unshrouded model ring-cascade reversers are illustrated in figure 21. The top portions of parts (a) and (b) show the Mach number profile in the reversed flow at two stations along the fairing. The bottom portions show the reversed-flow field at the station 4 nozzle diameters forward of the exhaust nozzle. The boundary of the reversed-flow field is the point at which the gage total pressure in the reversed flow is reduced to 1/2 percent of the exhaust-nozzle gage total pressure.

Figure 21(a) shows the reversed-flow characteristics of a reverser with six 60°-entry rings and a 50-percent-blockage flat-disk deflector. The flow is discharged in a continuous circumferential sheet, as with hemispherical target reversers (ref. 2), and in this case the reversed flow is attached to the fairing. The peak Mach number (about 0.85) occurs at the skin near the exhaust nozzle and decays to about 0.40 at the station 4 nozzle diameters forward of the exhaust nozzle.

3970

CH-2 back

The reversed-flow characteristics when the disk deflector is replaced with a 48-percent-blockage flat-bar deflector are shown in figure 21(b). The deflector is mounted with the long edge vertical. In this case the reversed-flow field is somewhat elongated, with the minor axis of the pattern parallel to the long edge of the deflector. This type of reversed-flow field is similar to the type produced by some of the basic cylindrical target reversers (ref. 3). The Mach number profiles through the major and minor axes of the pattern are similar in shape to those obtained with the disk deflector, but the magnitude is reduced in the plane of the minor axis (vertical plane).

The reversed flow was attached to the fairing for all the ring-cascade reversers reported herein, probably because the turning angle of the gas passing through the cascade was close to the cascade design turning angle (approx.  $160^\circ$ ). One method by which the attachment could probably be relieved consists of decreasing the cascade design turning angle, but at the same time the reverse-thrust ratio would be reduced. Further experimental work will possibly discover other methods of eliminating jet attachment.

Outside-circumference shrouds. - In some specific installations it may be necessary to eliminate reversed flow from as much as two opposite quadrants of the region around the fairing in order to protect portions of the aircraft, such as control surfaces. One method of doing this is by shrouding suitable portions of the cascade. As illustrated in figure 22(a), shrouds over the outside circumference of the cascade are effective in creating a sharply defined two-lobed reversed-flow field.

The effect on performance of this type of shrouding is shown in figure 22(b), in which reverse-thrust ratio is plotted against deflector blockage for both unshrouded reversers and shrouded reversers with  $\alpha_0$  of  $85^\circ$ . The shrouded configurations always produce less reverse thrust than the corresponding unshrouded ones. This occurs because the shrouds prevent some of the gas from turning and force it to exhaust to the rear. With shrouds, the bar deflectors produce more reverse thrust than the corresponding disk deflectors because, as shown by comparison of figures 21(a) and (b), the bar deflects less gas toward the region containing the shrouds than does the disk. Reverse-thrust ratio always increases as deflector blockage is increased (fig. 22(b)), and it appears that increasing the deflector blockage to values greater than 50 percent may result in further significant increases in reverse-thrust ratio for the shrouded configuration.

Tests with the  $60^\circ$ -entry single-curvature rings and  $\alpha_0 = 85^\circ$  shrouds showed that there was no deviation from the optimum ring spacing ratio as found for unshrouded cascades (see fig. 14).

Inside-circumference shrouds. - The reversed-flow fields created by reversers using a 48-percent-blockage bar deflector in which shrouds were placed on two opposite quadrants of the inside circumference of the cascade are shown in figure 23(a). When the shrouds are terminated at the leading edge of the first ring (top sketch), a reversed-flow field similar in shape to that produced by the unshrouded reverser of figure 21(b) is obtained. The flow at the top and bottom of the fairing was observed to be discharged from the pressure surface of the first ring.

In an attempt to improve their effectiveness, the shrouds were extended forward to the fairing. (At the same time, it was also necessary to increase the deflector spacing ratio about 30 percent over the value given in fig. 13 for both the 24- and 48-percent-blockage bar deflectors to maintain 100-percent air flow ratio.) The resulting reversed-flow field is shown in the bottom sketch of figure 23(a). Although the pattern is four-lobed, the top and bottom lobes are made up of low Mach number flow. This pattern might be acceptable in some installations. The gas in the top and bottom lobes was observed to have flowed circumferentially around the rings before being discharged from the vicinity of the vertical centerline of the cascade. A comparison of the reversed-flow fields in figures 22(a) and 23(a) shows that the outside-circumference shrouds are more effective than the inside-circumference shrouds of comparable included angle in removing reversed flow from portions of the fairing.

The effect on performance of this type of shrouding is given in figure 23(b), in which reverse-thrust ratio is plotted against deflector blockage. Performance of an unshrouded cascade is given for reference. Although reverse-thrust ratio increases as deflector blockage is increased, performance losses are again evident as a result of shrouding. The performance of the reversers is about the same whether the shrouds were terminated at the leading edge of the first ring or extended to the fairing.

Inside-outside shrouds. - The reversed-flow fields created by reversers in which shrouds are placed over both the inside and outside circumference of the cascade are shown in figure 24(a). The shrouds were "boxed in" with end plates to eliminate circumferential flow along the rings. When  $\alpha_1 = \alpha_0 = 60^\circ$  shrouds were used, the reversed-flow field (shown in the top sketch) that is obtained is similar in shape to that obtained with the unshrouded configuration of figure 21(b); however, although it is not shown in figure 24(a), the maximum Mach number of the flow in the vertical plane is less.

When the shrouds are enlarged so that  $\alpha_1 = \alpha_0 = 85^\circ$ , the reversed-flow boundary is changed to a sharply defined two-lobed pattern, as shown in the middle sketch. When portions of the inside shroud are removed so that  $\alpha_1$  is reduced to  $60^\circ$ , the sharply defined two-lobed pattern is maintained, as illustrated in the bottom sketch.

The performance of various reversers with this type of shrouding is shown in figure 24(b), in which reverse-thrust ratio is plotted against deflector blockage. Performance of an unshrouded cascade is again shown for reference. As noted previously, shrouding results in performance losses in each case. Generally, greater losses occur with the larger shrouds which produce the sharply defined two-lobed reversed-flow fields.

The maximum reverse-thrust ratio obtained with a configuration giving a sharply defined two-lobed reversed-flow field is 42 percent, using  $\alpha_1 = \alpha_0 = 85^\circ$  shrouds and a 48-percent-blockage bar deflector. The data of figure 24(b) indicate that this maximum value might be increased by use of a 48-percent-blockage bar deflector with  $\alpha_1 = 60^\circ$ ,  $\alpha_0 = 85^\circ$  shrouds or by increasing the blockage to more than 48 percent using  $\alpha_1 = \alpha_0 = 85^\circ$  shrouds.

Blade-angle reduction in portions of the cascade. - A method of altering the reversed-flow field without the use of mechanical shrouds consists of reducing the cascade blade angle in portions of the cascade. In the design tested, two opposite  $85^\circ$  sectors of each conventional  $0^\circ$ -entry ring were modified by bending the blade to discharge gas in a radial direction. The other sectors were unmodified, and no end plates were placed between sectors. A photograph of one of these rings is shown in figure 25, and a photograph of a reverser with these rings is shown in figure 26.

A reversed-flow field typical of this sort of configuration is shown in figure 27(a). Although the pattern is two-lobed, the effect is not as pronounced as obtained with some types of mechanical shrouds. However, the flow to  $35^\circ$  on either side of the vertical centerline is of low Mach number. In addition to the flow within the boundary shown, there is at the cascade a strong flow in a radial direction from the altered sectors of the cascade. In many installations, this radial flow would not strike parts of the aircraft.

The performance of reversers with this method of shrouding is shown in figure 27(b), in which reverse-thrust ratio is plotted against deflector blockage. Data are presented for several deflectors and various numbers of rings in the cascade. The performance of a cascade of six conventional rings is given for reference. The maximum reverse-thrust ratio obtained is 41 percent, which is comparable to that obtained with  $\alpha_1 = \alpha_0 = 85^\circ$  shrouds (fig. 24(b)). Generally, performance losses due to the alteration are not as severe as with the mechanically shrouded configurations; over 40-percent reverse-thrust ratio is obtained with 48-percent deflector blockage and five rings, and with 24-percent deflector blockage and six rings. Because the curves are relatively flat, it does not appear that additional blockage would significantly increase this performance.

### Thrust-Modulation Characteristics

Because of the high rotational inertia of the compressor and turbine in a turbojet engine, it would be desirable to control engine thrust by some means other than engine rotational speed during maneuvers such as landing. A thrust reverser which could modulate the thrust of the engine from full forward to reverse by changing the direction of the exhaust jet appears ideal. With such a reverser, aircraft could make landing approaches with engines running at full speed and with the required amount of forward or reverse thrust. Upon touchdown, only reverser actuation time would elapse before full reverse or forward thrust could be obtained, because the engine would already be at full speed.

The thrust-modulation performance of a typical shrouded ring-cascade reverser with two different deflectors is shown in figure 28. (The reversed-flow field for the reverser with 48-percent deflector blockage is illustrated in fig. 24(a).) As shown in the sketch, for this design the bar deflector was split along the minor axis and each half hinged at the cascade edge. The deflector halves were pivoted simultaneously into final position after the rings were in place.

In each case the thrust curve is smooth and continuous as the deflector is moved from the retracted position ( $\omega = 0^\circ$ ) to the maximum blockage position ( $\omega = 90^\circ$ ). No hysteresis effect was measured as the deflector was returned to the retracted position. The slope of the curve is always such that it was not difficult to set any desired value of thrust. There is no effect on air flow ratio at any deflector position.

Maximum reverse-thrust ratio occurs at or near the maximum deflector actuation angle and is 56 percent for the 48-percent-blockage deflector. When the deflector is retracted, about 80-percent forward thrust is obtained. It is necessary to retract the rings to obtain full forward thrust.

### SUMMARY OF RESULTS

Model ring-cascade thrust reversers were tested in quiescent air over a range of exhaust-nozzle pressure ratios up to 2.5. The models consisted of a mechanical deflector and a cascade of turning rings mounted aft of an exhaust nozzle with a  $7^\circ$  external fairing.

Deflector blockage, reverser working area, and ring spacing ratio were found to be the most significant variables affecting the performance of the basic configuration. The reverse-thrust ratio increased as deflector blockage increased. Ring-cascade reversers required about twice as much working (total projected) area to produce maximum reverse-thrust



ratio as hemispherical target reversers. An optimum ring spacing ratio was found for each of three ring cross-sectional designs tested. Other geometric variables, such as deflector shape, deflector spacing ratio, ring cross-sectional design, and first-ring spacing ratio, did not appreciably affect reverse-thrust ratio over a considerable range of practical values. For all reversers tested, maximum reverse-thrust ratio occurred at or near the minimum deflector spacing required for 100-percent air flow ratio. Reverse-thrust ratios up to 68 percent can be obtained using 50-percent deflector blockage and near-optimum values of other geometric design parameters.

The basic reverser was found to give a near-circular reversed-flow boundary, and the reversed flow was attached to the fairing in all cases for the ring cross-sectional designs tested. It was possible to obtain a sharply defined two-lobed reversed-flow boundary by suitably shrouding portions of the cascade, but the reverse-thrust ratio fell off appreciably when this was done. For the case in which reversed flow was completely blocked from approximately two quadrants of the fairing, a maximum reverse-thrust ratio of 42 percent was measured.

The modulation characteristics of a shrouded reverser were found to be satisfactory.

The results of this investigation showed that a ring-cascade reverser producing over 40-percent reverse-thrust ratio could be built having a sharply defined two-lobed reversed-flow field, satisfactory modulation characteristics, a length in the order of 1 to  $1\frac{1}{4}$  exhaust-nozzle diameters, and no indication of effect on engine performance.

Lewis Flight Propulsion Laboratory  
National Advisory Committee for Aeronautics  
Cleveland, Ohio, August 10, 1956

## APPENDIX A

## SYMBOLS

A	area or projected area
D	diameter
F	thrust
l	axial distance between leading edge of first ring and exhaust-nozzle exit
N	number of rings
P	total pressure
p	static pressure
S	axial distance between corresponding points on adjacent rings
w	air flow, lb/sec
x	axial distance from exhaust-nozzle exit to deflector (fig. 2)
y	geometric dimension on deflector
$\alpha$	included angle of shroud, deg
$\delta$	ratio of total pressure at nozzle inlet to absolute pressure at NACA standard sea-level conditions
$\eta_R$	reverse-thrust ratio
$\theta$	ratio of total temperature at nozzle inlet to absolute temperature at NACA standard sea-level conditions
$\omega$	deflector actuation angle, deg

## Subscripts:

d	deflector
F	forward
i	inside
j	jet

n exhaust-nozzle exit  
o outside  
R reverse  
r reverser ring  
O ambient

## APPENDIX B

## DEFINITIONS

Deflector blockage	$A_d/A_n$
Deflector spacing ratio	$x/D_n$
Ring spacing ratio	$S/D_n$
First-ring spacing ratio	$l/D_n$
Reverser working-area ratio	$(NA_r + A_d)/A_n$
Reverse-thrust ratio $\eta_R$	$\left[ \frac{(F_j/\delta_n)_R}{(F_j/\delta_n)_F} \right] (P_n/p_0)_R = (P_n/p_0)_F$
Air flow ratio	$\left[ \frac{(w_n \sqrt{\theta})_R}{(w_n \sqrt{\theta})_F} \right] (P_n/p_0)_R = (P_n/p_0)_F$

## REFERENCES

1. Sutter, Joseph: Reverse Thrust for Jet Transports. Paper presented at meeting SAE, New York (N.Y.), Apr. 12-15, 1954.
2. Steffen, Fred W., McArdle, Jack G., and Coats, James W.: Performance Characteristics of Hemispherical Target-Type Thrust Reversers. NACA RM E55E18, 1955.
3. Steffen, Fred W., and McArdle, Jack G.: Performance Characteristics of Cylindrical Target-Type Thrust Reversers. NACA RM E55I29, 1956.
4. Henzel, James G., Jr., and McArdle, Jack G.: Preliminary Performance Data of Several Tail-Pipe-Cascade-Type Model Thrust Reversers. NACA RM E55F09, 1955.
5. Povolny, John H., Steffen, Fred W., and McArdle, Jack G.: Summary of Scale-Model Thrust-Reverser Investigation. NACA TN 3664, 1956.

6. Iserland, K.: Braking the Landing Run of Jet Aircraft by Thrust Deviation. Interavia, vol. VIII, no. 3, 1953, pp. 151-154.
7. Bertin, J., Kadosch, M., and Maunoury, F.: Jet Deflection. Shell Aviation News, no. 205, July 1955, pp. 22-24.

3970

TABLE I. - PERFORMANCE OF SIGNIFICANT RING-CASCADE




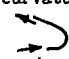
Configuration	Ring shape	Ring inside-diameter ratio, $D_{i,r}/D_n$	Ring outside-diameter ratio, $D_{o,r}/D_n$	Number of rings, N	Ring spacing ratio, $S/D_n$	First-ring spacing ratio, $z/D_n$	Deflector shape
1	Semicircular 	0.81	1.18	12	0.094	0.125	Flat plate
2		↓	↓	↓	.125	↓	↓
3		↓	↓	↓	.156	↓	↓
4		1.00	1.38	↓	.125	↓	↓
5		1.00	1.38	↓	.125	↓	Flat plate
6		1.00	1.38	↓	.094	↓	↓
7		1.25	1.62	↓	.094	↓	↓
8		1.25	1.62	↓	.125	↓	↓
9		.67	1.04	↓	↓	.38	↓
10		.67	1.04	↓	↓	↓	↓
11		1.00	1.38	6	.156	.188	Bar
12		↓	↓	6	.25	↓	↓
13		↓	↓	10	.188	↓	↓
14		↓	↓	8	.156	↓	↓
15		↓	↓	8	.25	↓	↓
16		↓	↓	10	.188	↓	↓
17		↓	↓	6	.156	↓	↓
18		↓	↓	↓	.188	↓	↓
19		↓	↓	↓	.25	↓	↓
20		↓	↓	10	.188	↓	↓
21		1.25	1.62	6	.125	↓	↓
22		↓	↓	↓	.156	↓	↓
23		↓	↓	↓	.188	↓	↓
24		↓	↓	↓	.125	↓	↓
25		↓	↓	↓	.156	↓	↓
26		↓	↓	↓	.188	↓	↓
27		↓	↓	↓	.125	↓	↓
28		↓	↓	↓	.156	↓	↓
29		↓	↓	↓	.188	↓	↓
30	60° Entry, single curvature 	1.05	1.49	8	0.094	0.275	Flat plate
31		↓	↓	6	.156	.40	Disk
32		↓	↓	↓	↓	↓	Vented disk
33		↓	↓	↓	↓	↓	Rectangle
34		↓	↓	↓	↓	↓	Bar
35		↓	↓	↓	↓	↓	↓
36		↓	↓	↓	↓	↓	Disk
37		↓	↓	↓	↓	↓	Rectangle
38		↓	↓	↓	.14	↓	Bar
39		↓	↓	↓	.156	↓	Disk
40		↓	↓	↓	.188	↓	Rectangle
41		↓	↓	5	.156	↓	Bar
42		↓	↓	4	↓	↓	Disk
43		↓	↓	3	↓	↓	↓
44		↓	↓	6	↓	↓	↓
45		↓	↓	↓	↓	.28	↓
46		↓	↓	↓	↓	.40	Rectangle
47		↓	↓	↓	↓	↓	Bar
48		↓	↓	↓	↓	↓	↓
49		↓	↓	↓	↓	↓	↓
50		↓	↓	↓	↓	↓	Disk
51		↓	↓	↓	↓	↓	Rectangle
52		↓	↓	↓	↓	↓	Bar
53		↓	↓	↓	.188	↓	Bar
54		↓	↓	↓	↓	↓	Disk
55		↓	↓	↓	↓	↓	Bar
56		↓	↓	↓	↓	↓	Bar
57		Varied	Varied	↓	↓	↓	Disk
58		↓	↓	↓	↓	↓	Bar
59		↓	↓	↓	↓	↓	Bar
60		↓	↓	↓	↓	↓	Bar
61	60° Entry, double curvature 	1.08	1.28	10	0.11	0.31	Disk
62		↓	↓	↓	↓	↓	Vented disk
63		↓	↓	↓	↓	↓	Rectangle
64		↓	↓	↓	↓	↓	Bar
65		↓	↓	↓	↓	↓	Disk
66		↓	↓	↓	.125	↓	Rectangle
67		↓	↓	↓	.094	↓	Bar
68		↓	↓	↓	.125	↓	Disk
69		↓	↓	↓	.125	↓	Rectangle
70		↓	↓	↓	.125	↓	Bar
71		↓	↓	8	.11	↓	Disk
72		↓	↓	↓	↓	↓	↓
73		↓	↓	↓	↓	↓	↓
74		↓	↓	↓	↓	↓	Bar
75		↓	↓	↓	↓	↓	Disk





TABLE I. - Concluded. PERFORMANCE OF SIGNIFICANT RING-CASCADE

Configuration	Ring shape	Ring inside-diameter ratio, $D_{1,r}/D_n$	Ring outside-diameter ratio, $D_{o,r}/D_n$	Number of rings, $N$	Ring spacing ratio, $S/D_n$	First-ring spacing ratio, $1/D_n$	Deflector shape		
76	0° Entry, single curvature 	1.05	1.49	6	0.188	0.31	Disk		
77					.188		Rectangle		
78					.25		Bar		
79					↓		Vented bar		
80							Disk		
81					.188		Rectangle		
82					.25		Bar		
83					.188		Disk		
84					.25		Rectangle		
85					.25		Bar		
86	↓				.25	↓	Wedge		
87					.25		Wedge		
88					.188		Disk		
89					.188		Bar		
90					.25		Bar		
91				2	.25		Bar		
92					.25				
93				↓	.188		↓		
94				6	.25				
95				6	.25				
96	↓			6	.25		↓		
97				↓					
98									
99				4	Disk				
100				4	Disk				
101				4			Bar		
102									
103				6	↓				
104				↓			Disk		
105							Disk		
106	↓						Bar		
107							↓		
108									
109				Varied			↓		
110									
111				3			↓		
112				3					
113				6					
114									
115	0° Entry, split	Varied	↓	↓	↓	↓	Disk		
116							Disk		
117							Bar		

## Notes:

1. Deflector blockage behind last ring in order to get maximum  $\eta_R$ .
2. Included in performance plots (figs. 10 to 18, 20 to 24, 27, and 28).
3. Curves of  $\eta_R$  against  $S/D_n$  similar to those shown in fig. 14.
4. Deflector not illustrated in fig. 4. Other dimension found from  $A_d/A_n$  and  $y/D_n$ .
5.  $\alpha_0 = 85^\circ$  Shrouds on two opposite sectors of cascade. Shrouds extended forward to fairing.
6.  $\alpha_1 = \alpha_0 = 85^\circ$  Shrouds on two opposite sectors of cascade. Inside-circumference shrouds terminated at leading edge of first ring. Outside-circumference shrouds extended forward to fairing. Shrouds "boxed in" with end plates.
7. See fig. 19.
8.  $\alpha_1 = 90^\circ$  Shrouds on two opposite sectors of cascade.
  - (a) Shrouds extended forward to fairing.
  - (b) Shrouds terminated at leading edge of first ring.
9. Shrouds on two opposite sectors of cascade. Outside-circumference shrouds extended forward to fairing. Inside-circumference shrouds terminated at leading edge of first ring. Shrouds "boxed in" with end plates.
  - (a)  $\alpha_1 = \alpha_0 = 80^\circ$ .
  - (b)  $\alpha_1 = 80^\circ$ ,  $\alpha_0 = 85^\circ$ .
10. Modulation characteristics obtained.  $\eta_R$  tabulated for  $\alpha = 90^\circ$ .
11. Two  $85^\circ$  sectors of ring bent to discharge gas in radial direction. See fig. 25.

## THRUST REVERSERS AT EXHAUST-NOZZLE PRESSURE RATIO OF 2.0

Deflector blockage, $A_d/A_n$ , percent	$y/D_n$ or $D_d/D_n$	Deflector spacing ratio, $x/D_n$	Air flow ratio, percent	Reverse-thrust ratio, $\eta_R$ , percent	See note -	Remarks
16 ↓ 25	0.41 .25 .125 .125 .50	0.405 ↓ .445	100 ↓	38 43 46 51 47	3 3,4 2 3 2	Max. $\eta_R$ for $0.156 < S/D_n < 0.28$ ↓
24 24 50 48 48	.31 .188 .71 .44 .38	.445 ↓ .53 ↓	↓	60 53 68 65 64	3,4 2 3 3,4 2	
24 24 16 48 16	.188 .188 .41 .38 .125	.36 .445 .405 .53 .405	99 100 ↓	51 49 34 64 44	--- --- --- 2 ---	(Max. $\eta_R$ for 100% air flow ratio for $0.27 < x/D_n < 1.0$ ) Max. $\eta_R$ for $0.125 < i/D_n < 0.31$ Max. $\eta_R$ for $0 < i/D_n < 0.44$ ↓
48 24 48 ↓	.38 .188 .38 ↓	.53 .445 .53 ↓	↓	-9 -51 -20 92 100	2 ↓ 8(a) 2,8(a)	See fig. 17 ↓
24 48 24 25 50	.188 .38 .188 .50 .71	.56 .56 .47 .47 .56	100 ↓	13 52 4 -8 25	2,8(a) 2,8(b) 2,8(b) 6 6	
48 24 48 25 50	.38 .188 .38 .50 .71	.56 .47 .56 .47 .56	↓	34 -5 42 -10 25	2,6 ↓	
48 24 24 48 24	.38 .188 .188 .38 .188	.54 ↓ ↓ .53 .445	↓	56 27 11 42 41	2,9(a),10 2,9(a),10 2,9(b),10 2,11 2,11	
48 24 16 16 48 24 0	.38 .188 .125 .41 .71 .188 ---	.53 .445 .405 .405 .53 .445 ---	↓	17 -6 31 14 33 44 -45	11 11 2,11 ↓ 2,7 2,7	Max. $\eta_R$ for $0.188 < S/D_n < 0.314$ Max. $\eta_R$ for $0.188 < S/D_n < 0.314$

3970

CH-4

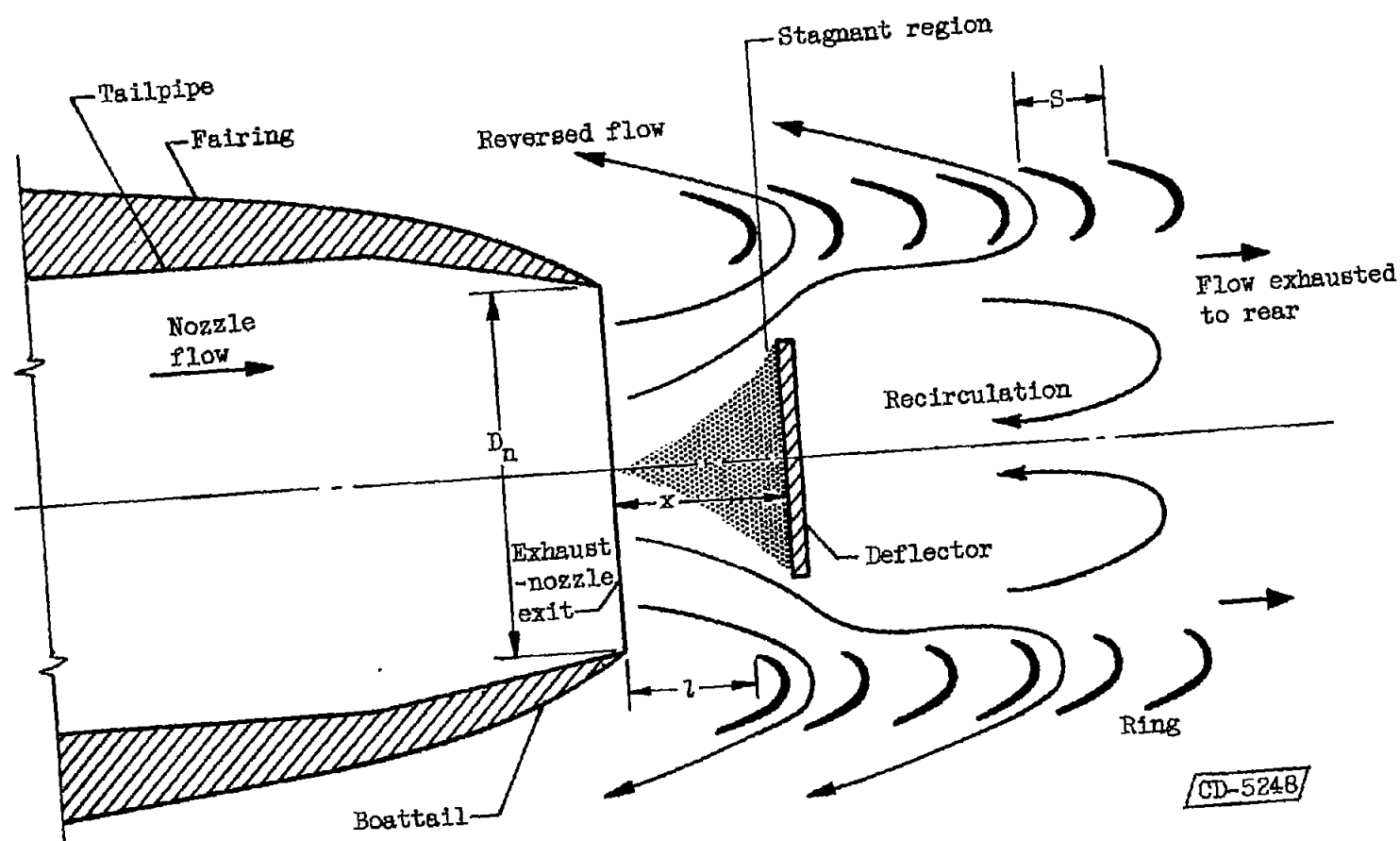
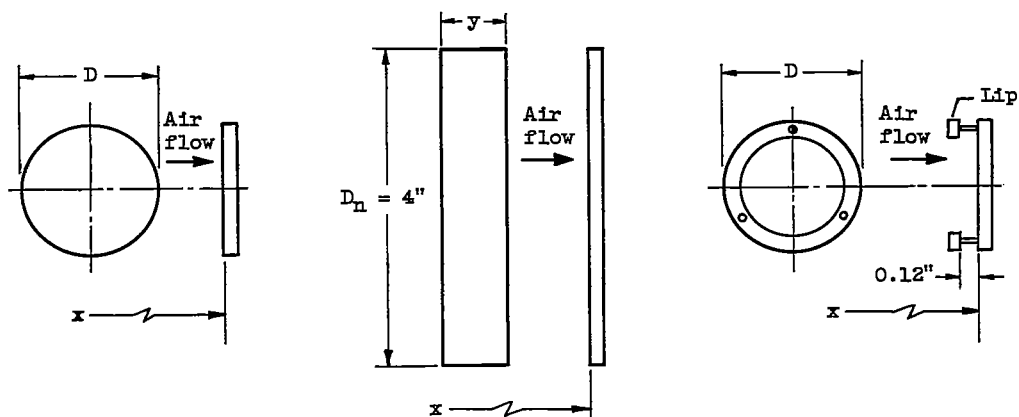


Figure 1. - Schematic sketch of principle of operation of ring-cascade reverser with mechanical deflector.

3970



D, in.	$A_d/A_n$ , percent
1.62	16
2.00	25
2.83	50

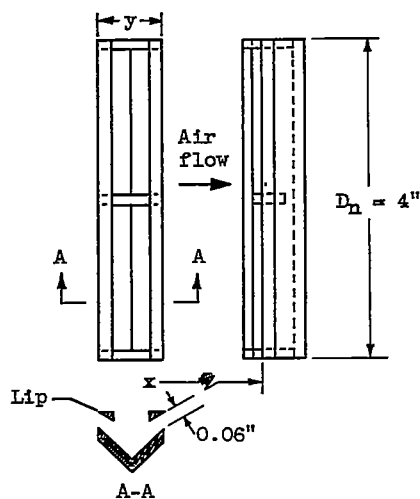
(a) Flat disk.

y, in.	Deflector blockage, $A_d/A_n$ , percent
$\frac{1}{2}$	16
$\frac{3}{4}$	24
$1 \frac{1}{2}$	48

(b) Flat bar.

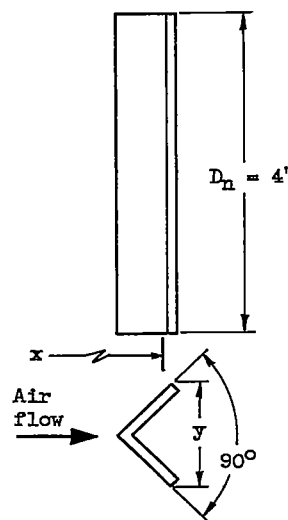
D, in.	$A_d/A_n$ , percent
1.62	16

(c) Vented disk.



y, in.	$A_d/A_n$ , percent
$\frac{1}{2}$	16

(d) Vented bar.



y, in.	$A_d/A_n$ , percent
$\frac{3}{4}$	25

(e) Wedge bar.

CD-5249

Figure 2. - Deflector designs tested.

CH-4 back

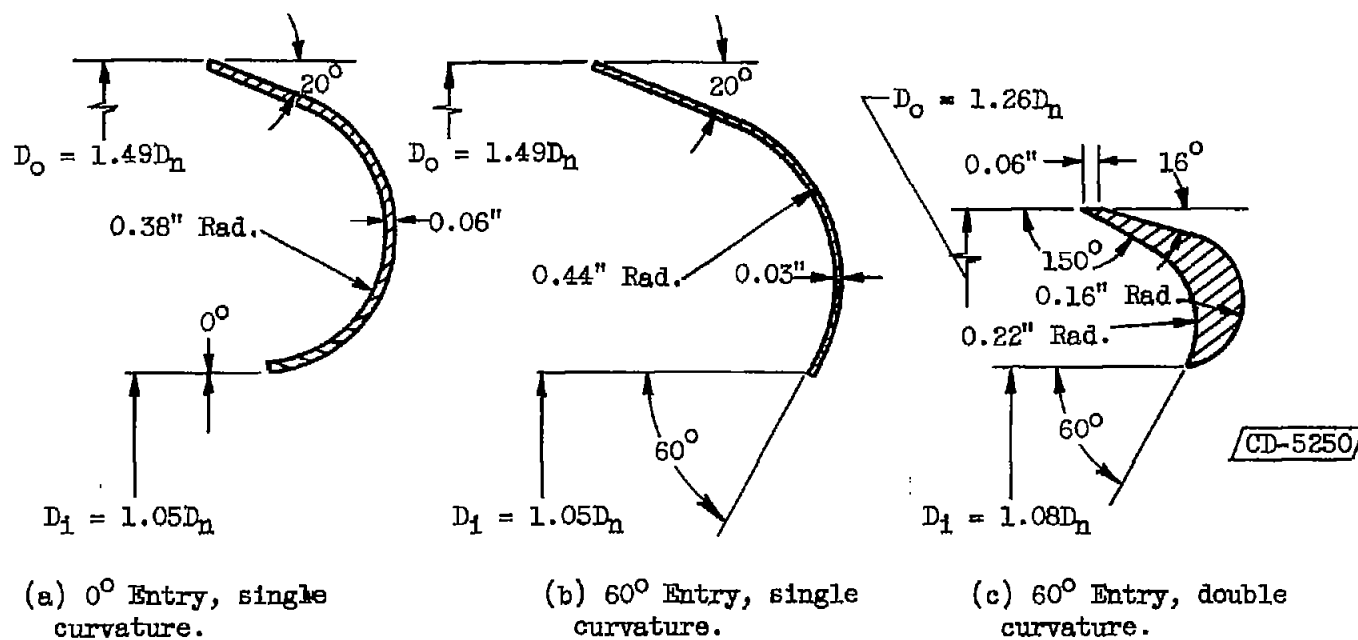


Figure 3. - Ring cross-sectional designs tested.

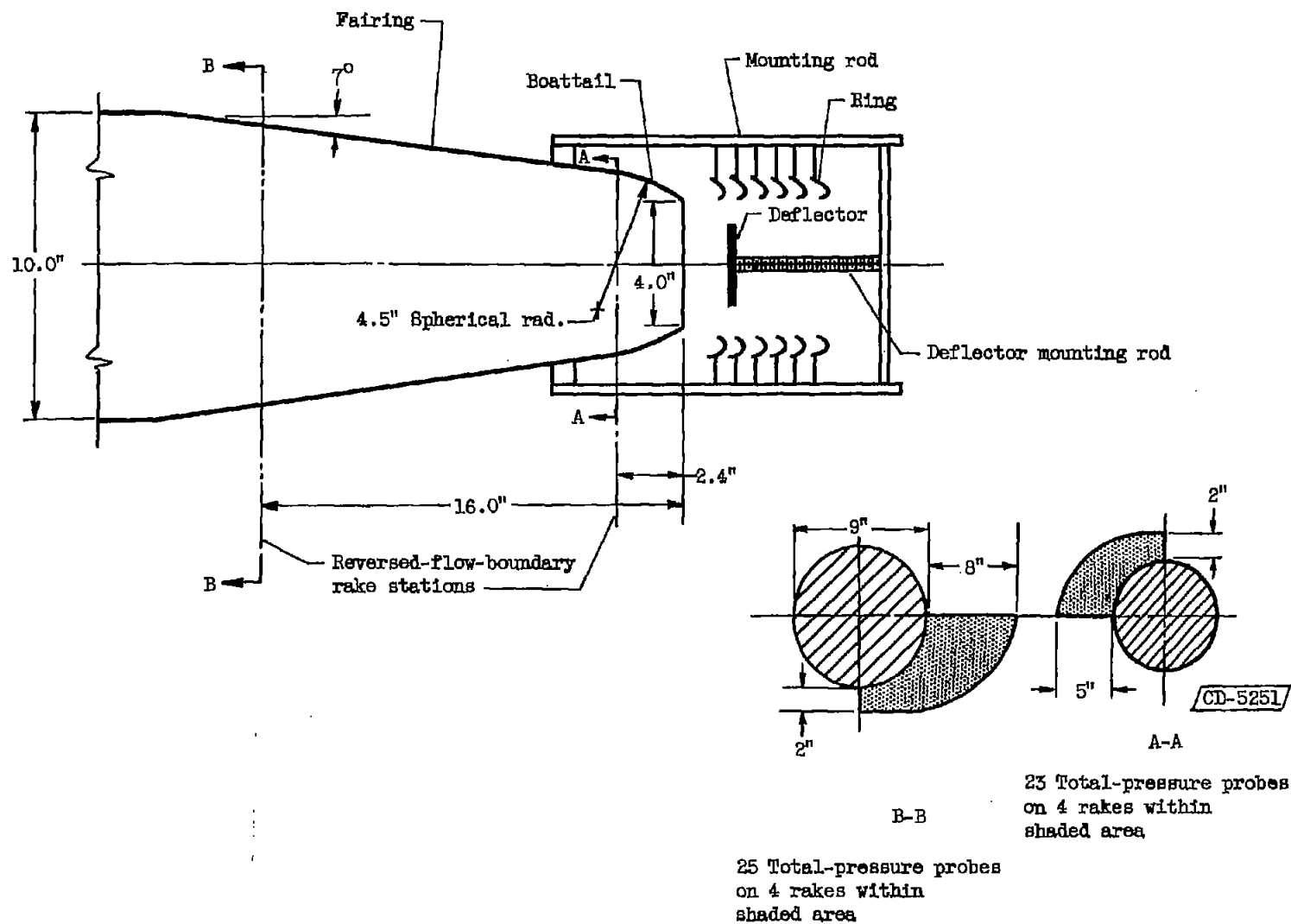


Figure 4. - Schematic sketch of model ring-cascade thrust reverser.

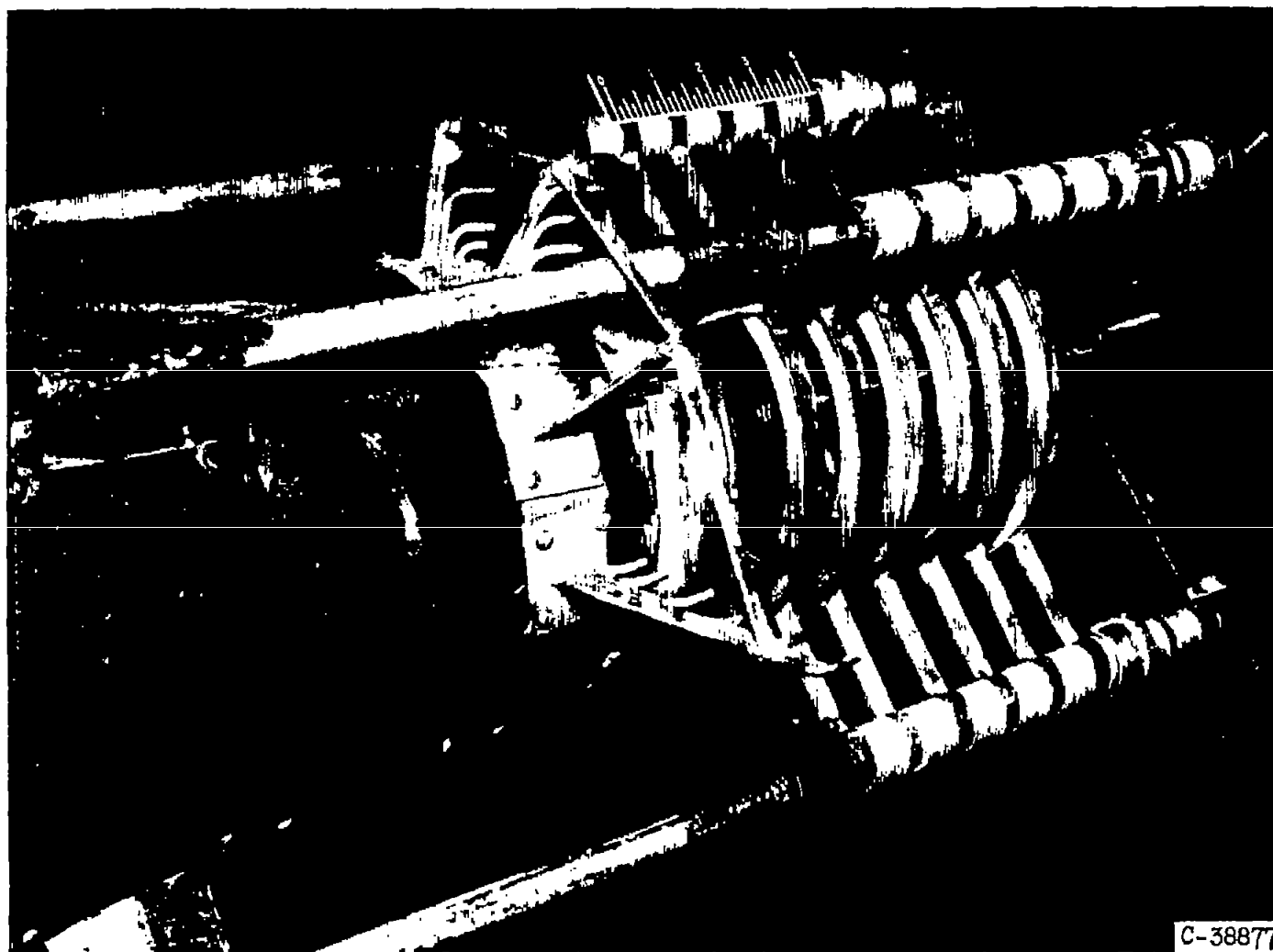
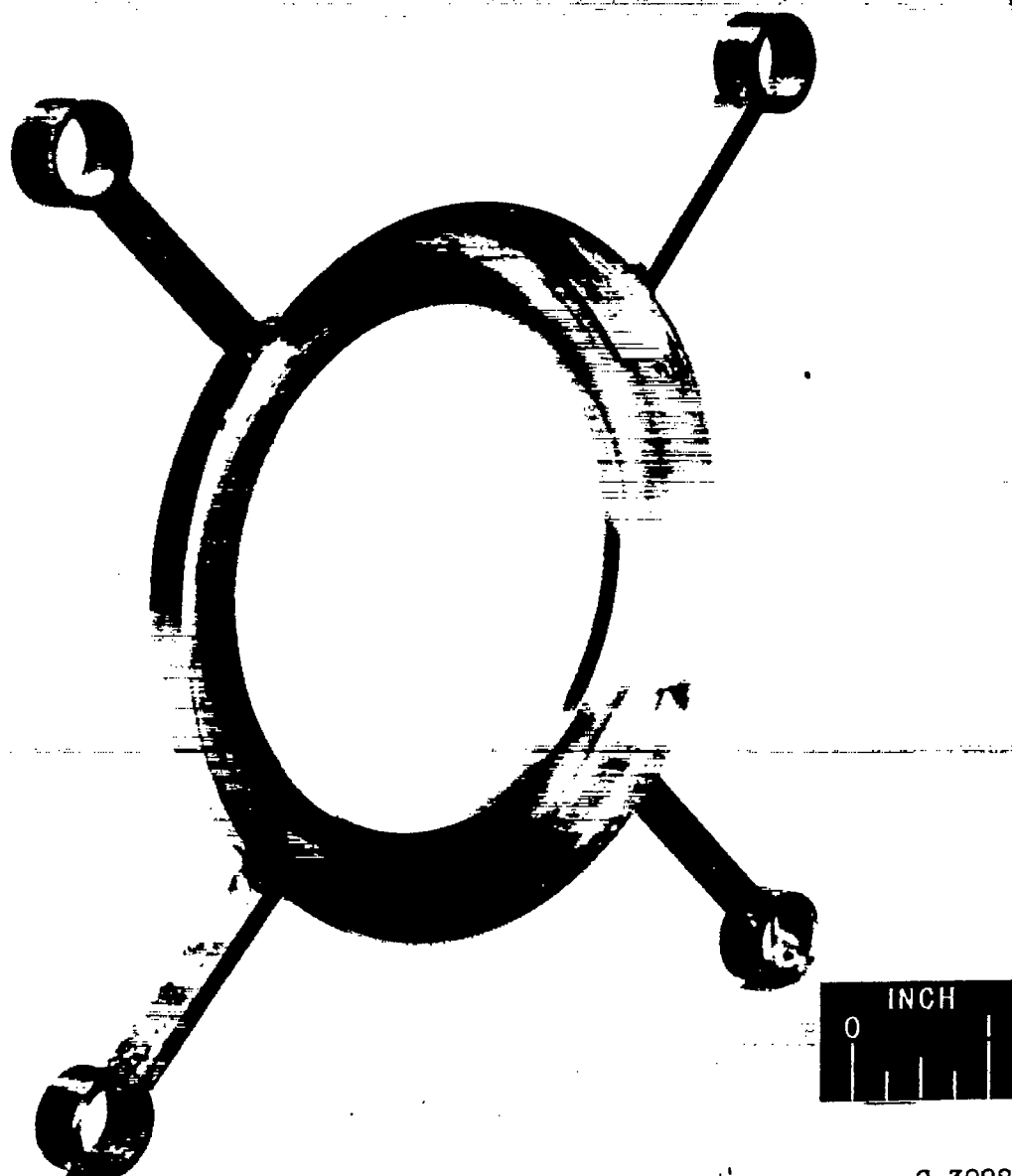


Figure 5. - Three-quarter view of typical ring-cascade reverser.

3970



C-39982

Figure 6. - Three-quarter view of typical ring used in tests.



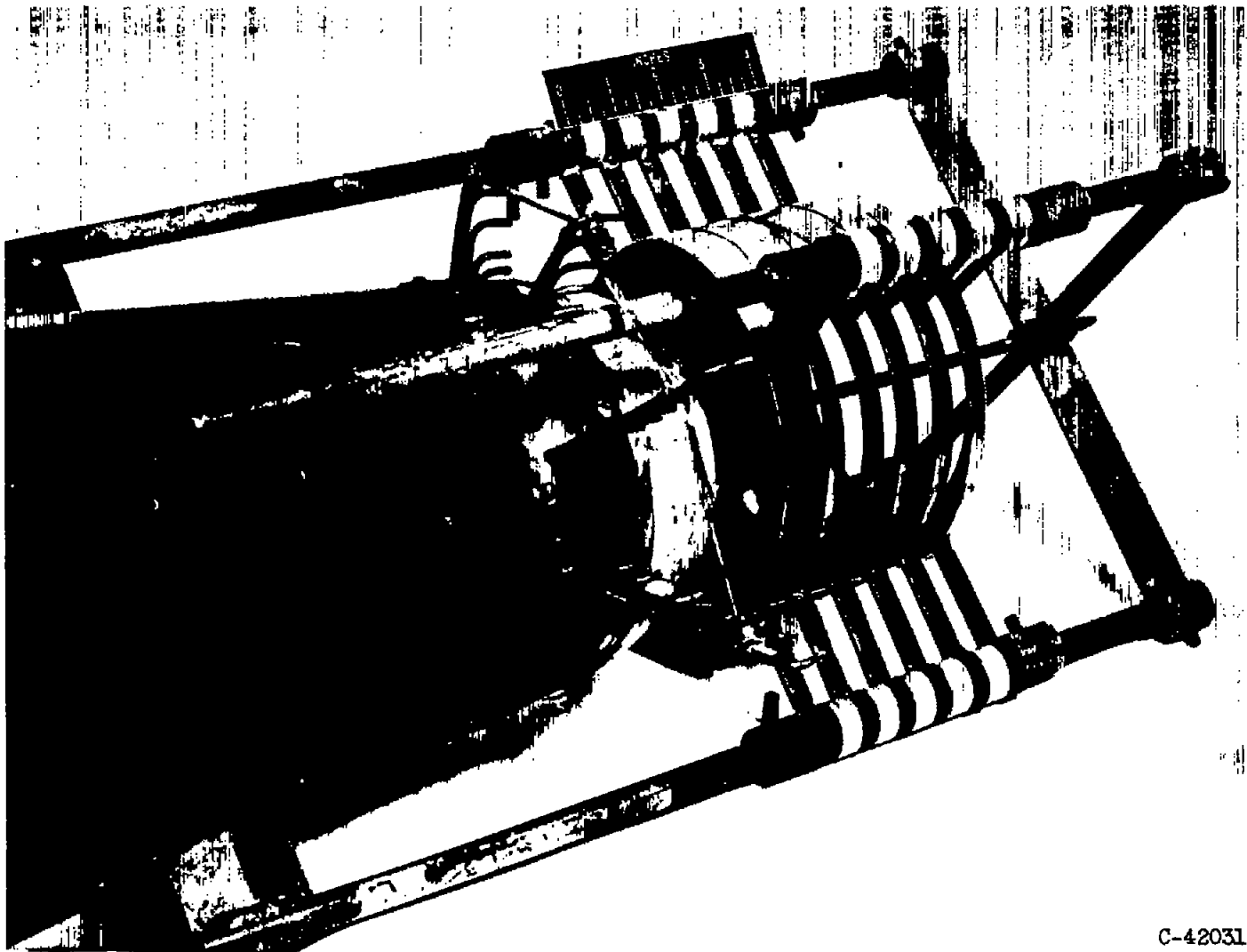


Figure 7. - Ring-cascade reverser with outside-circumference shrouds.

C-42031

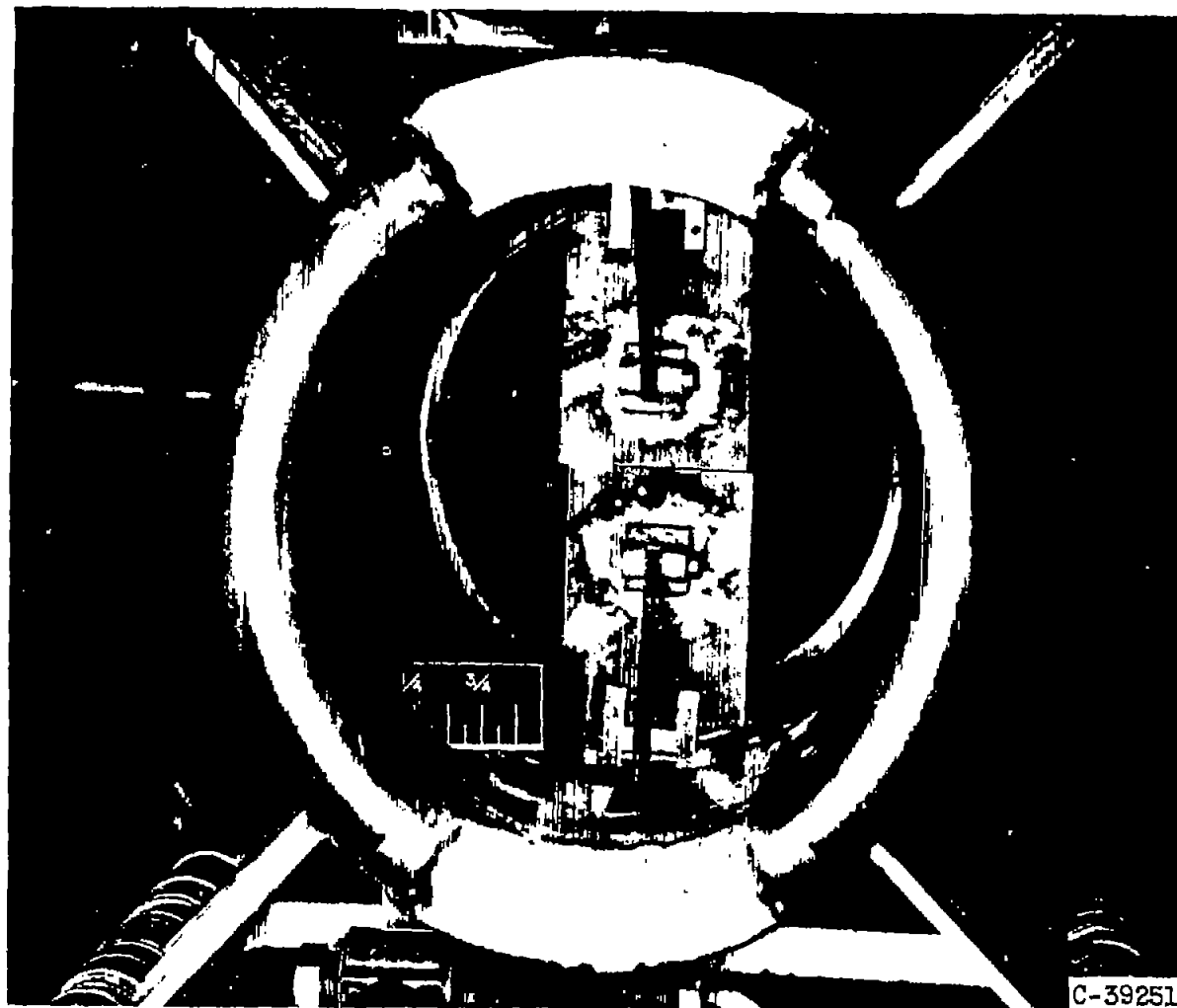


Figure 8. - Rear view of adjustable model used to determine modulation characteristics.

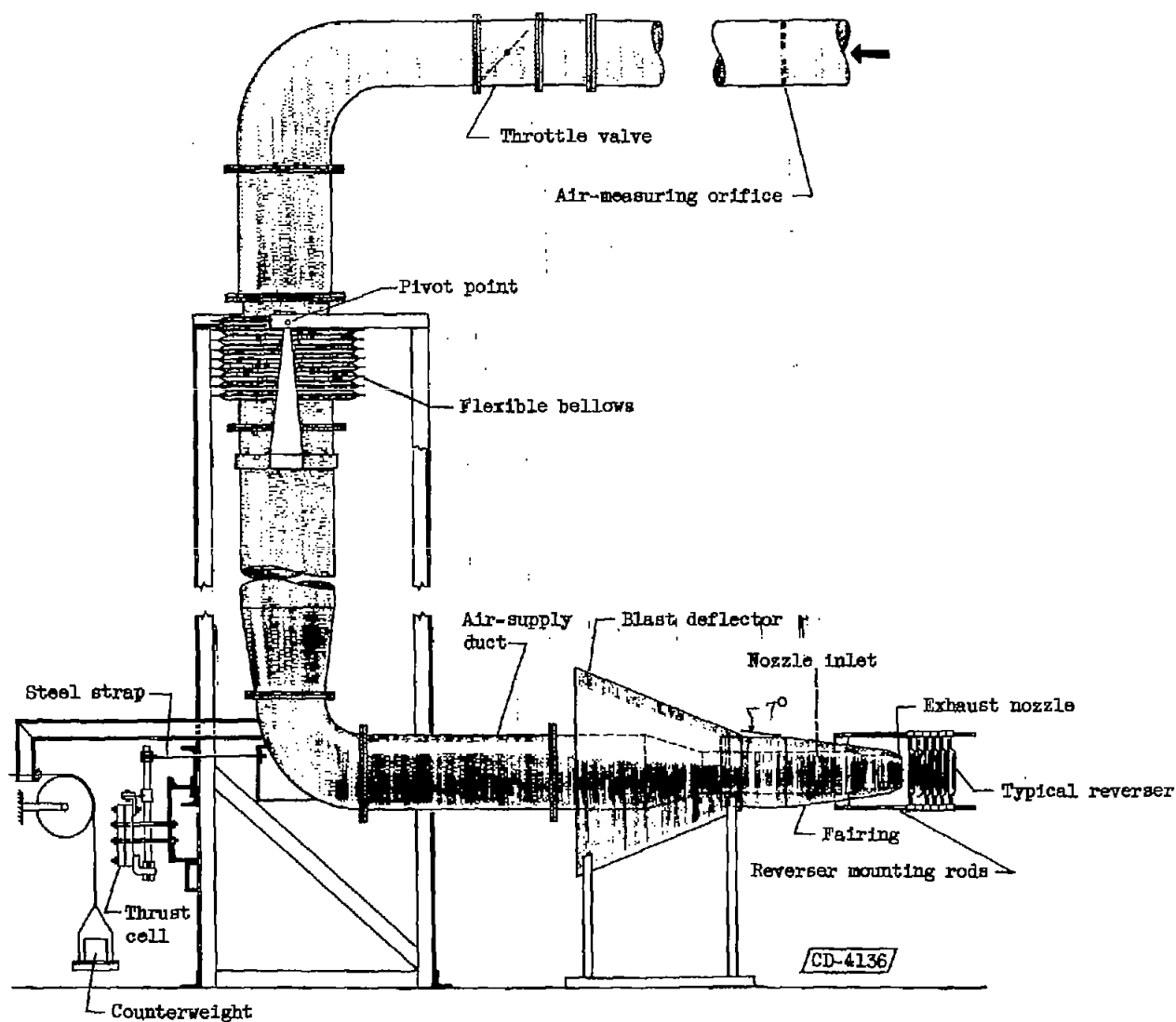


Figure 9. - Schematic diagram of setup for thrust-reversal investigation.

3970

CH-5 back

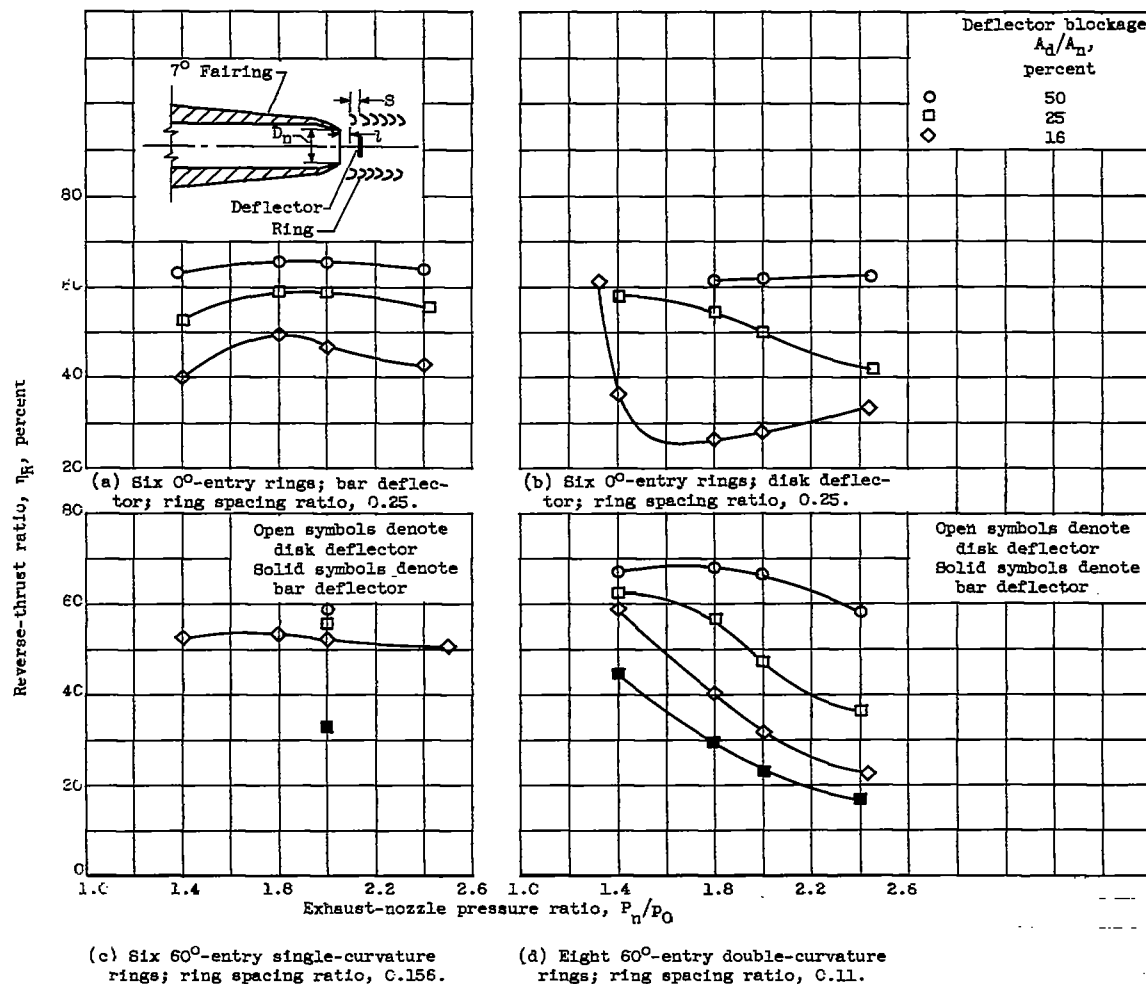


Figure 10. - Effect of nozzle pressure ratio on reverse-thrust ratio. First-ring spacing ratio, about 0.35; air flow ratio at  $P_n/P_0 \geq 2.0$ , 100 percent.

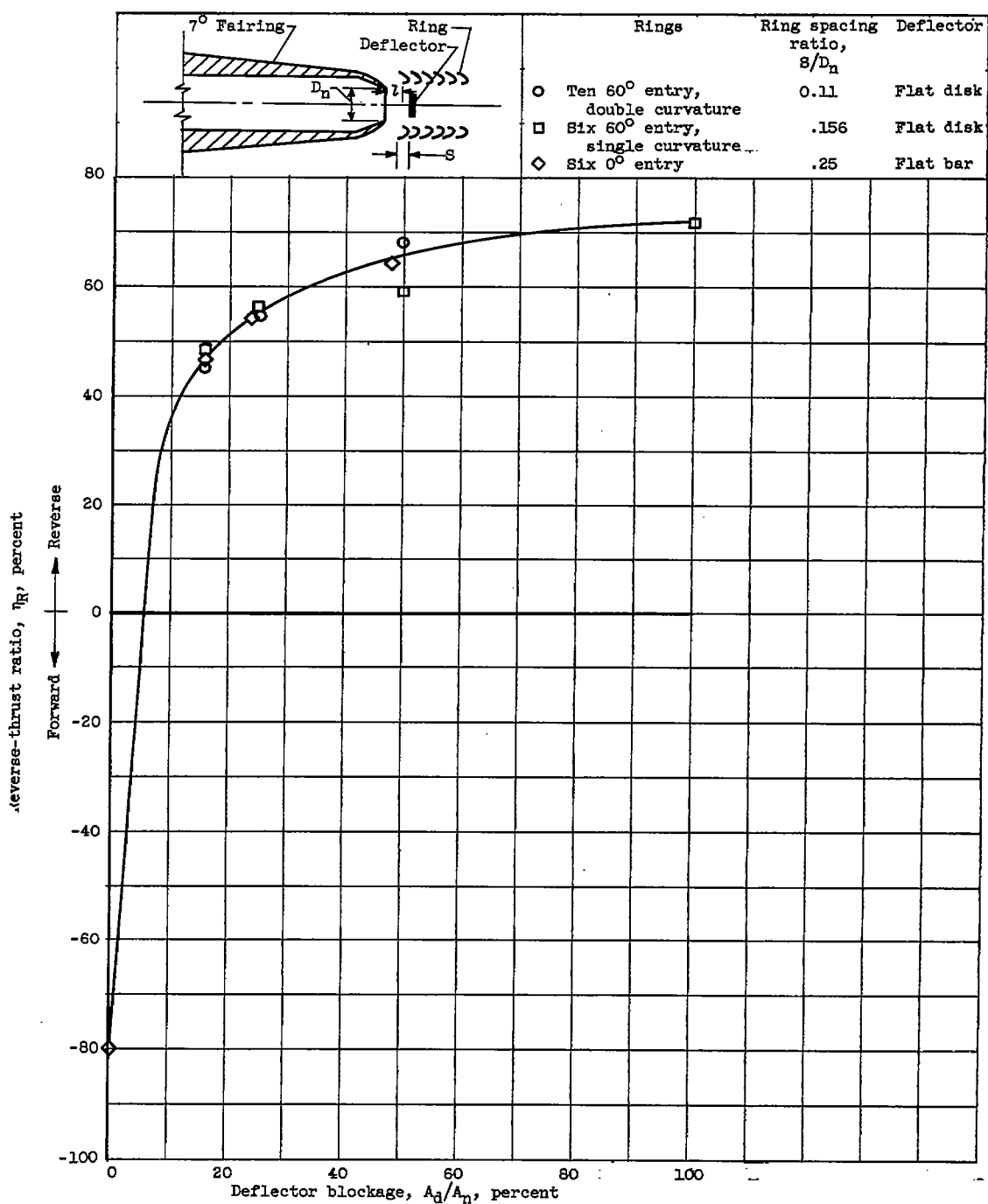


Figure 11. - Effect of deflector blockage on reverse-thrust ratio. First-ring spacing ratio, about 0.35; minimum deflector spacing ratio for 100 percent air flow ratio; exhaust-nozzle pressure ratio, 2.0.

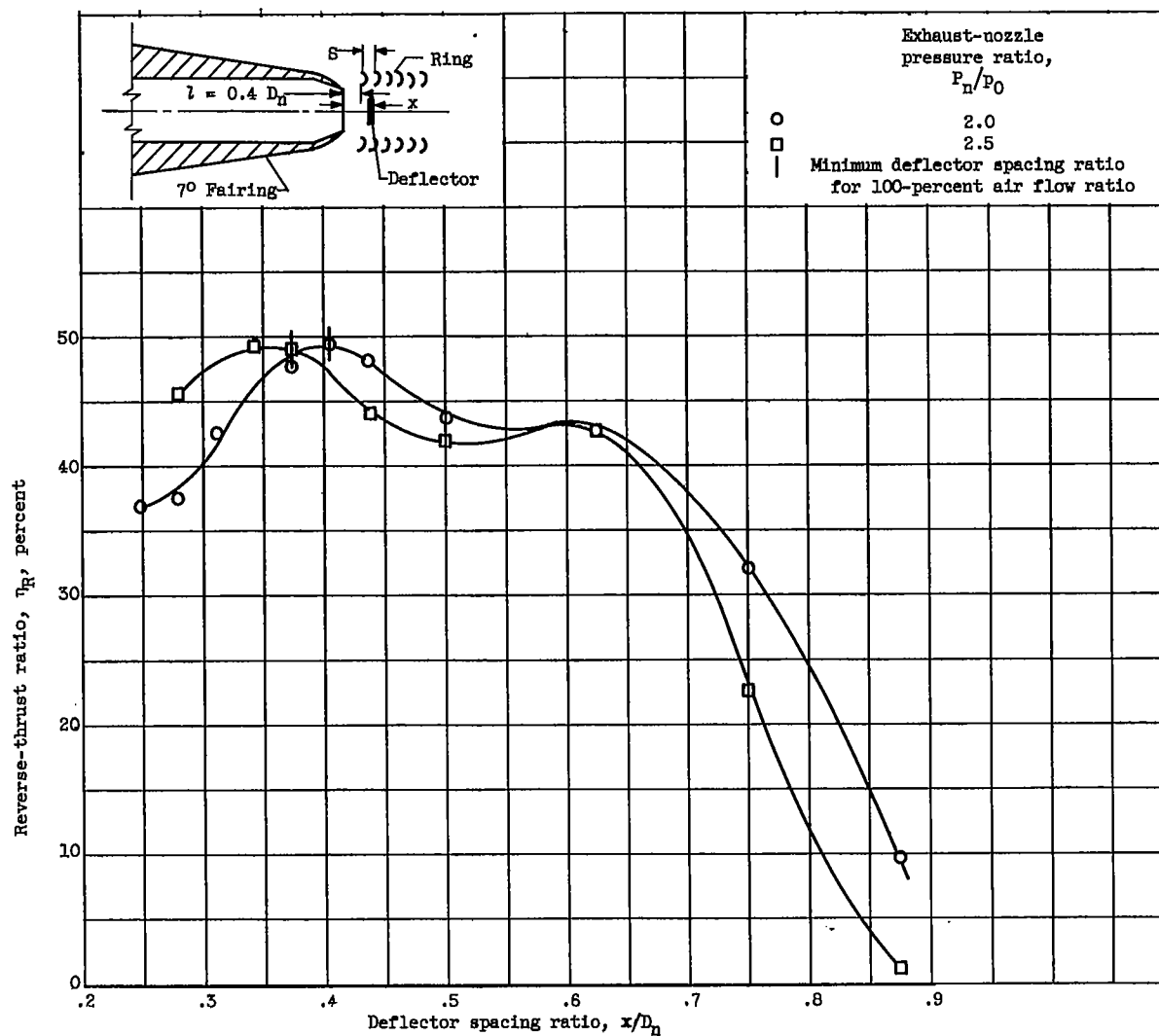


Figure 12. - Effect of deflector spacing ratio on reverse-thrust ratio with 16-percent-blockage flat-disk deflector. Six 60°-entry rings; ring spacing ratio, 1.56.

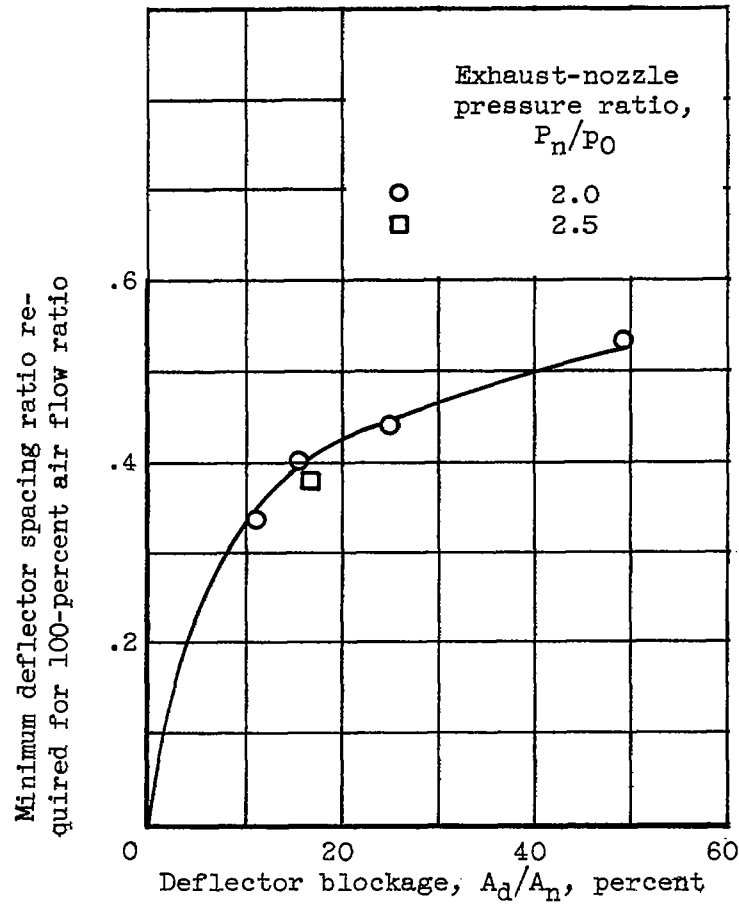


Figure 13. -- Minimum deflector spacing ratio required for 100-percent air flow ratio for various deflectors.

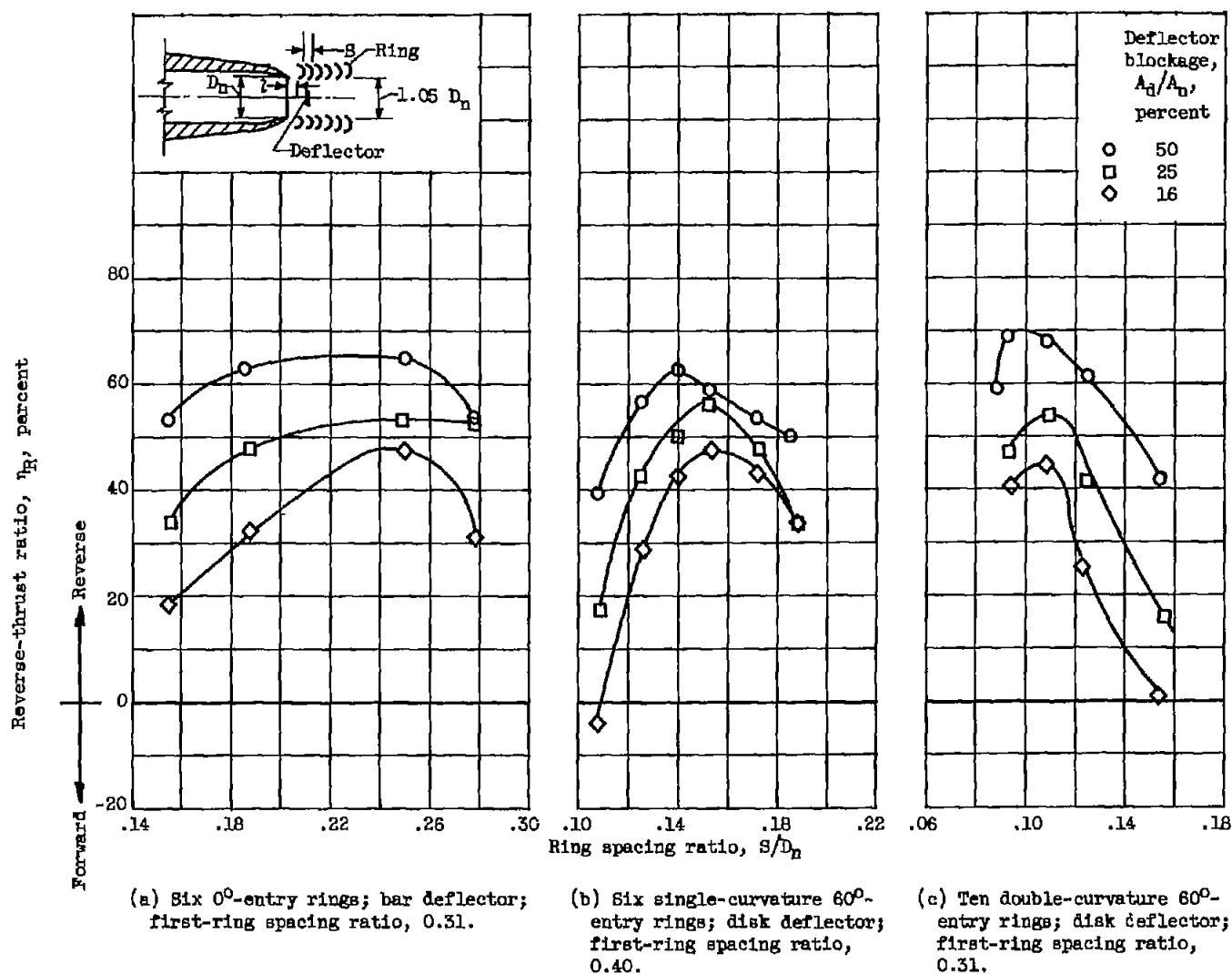


Figure 14. - Effect of ring spacing ratio on reverse-thrust ratio. Air flow ratio, 100 percent; exhaust-nozzle pressure ratio, 2.0.



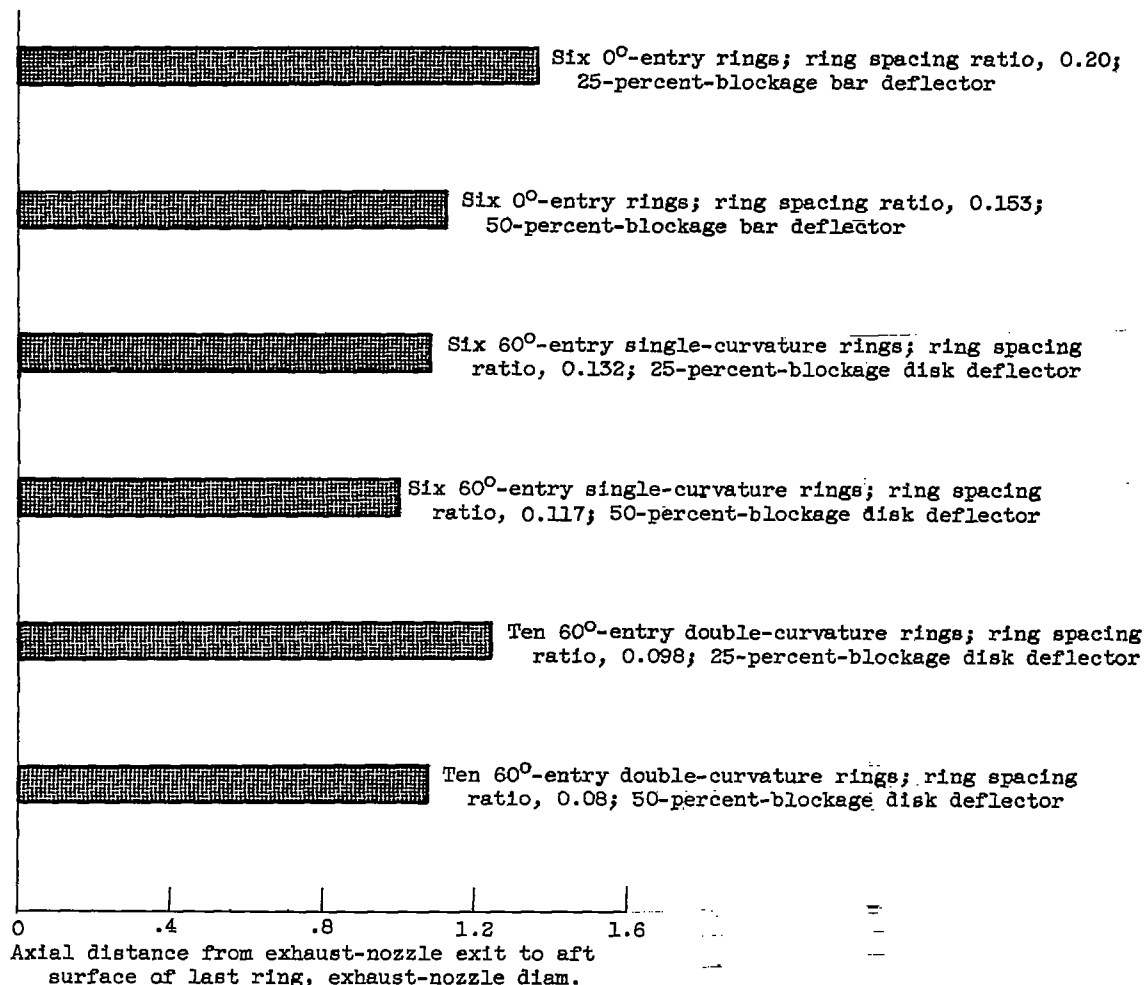


Figure 15. - Comparison of cascade lengths required to give 50-percent reverse-thrust ratio. First-ring spacing ratio, about 0.35; air flow ratio, 100 percent; exhaust-nozzle pressure ratio, 2.0.

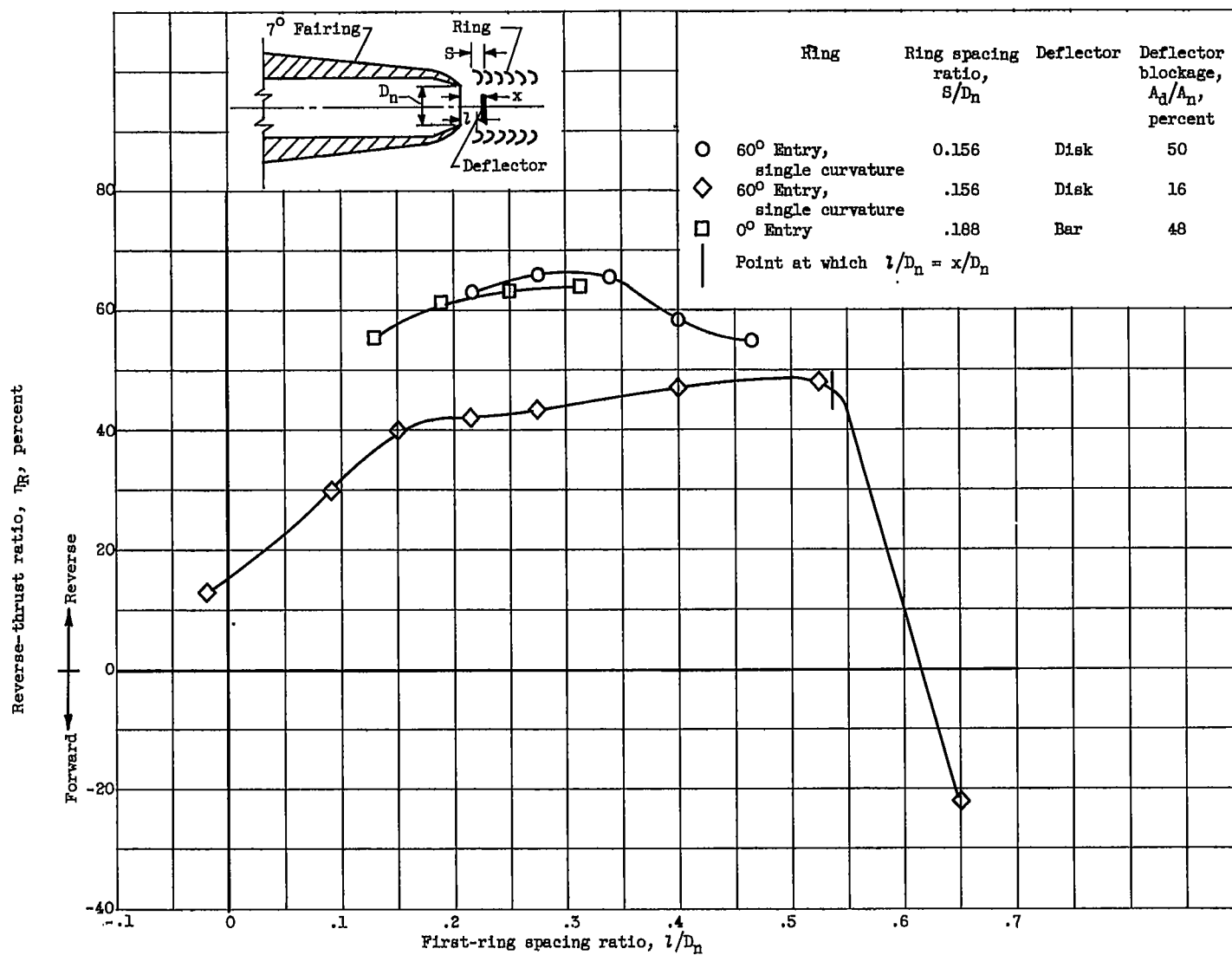


Figure 16. - Effect of first-ring spacing ratio on reverse-thrust ratio. Six rings; air flow ratio, 100 percent; exhaust-nozzle pressure ratio, 2.0.

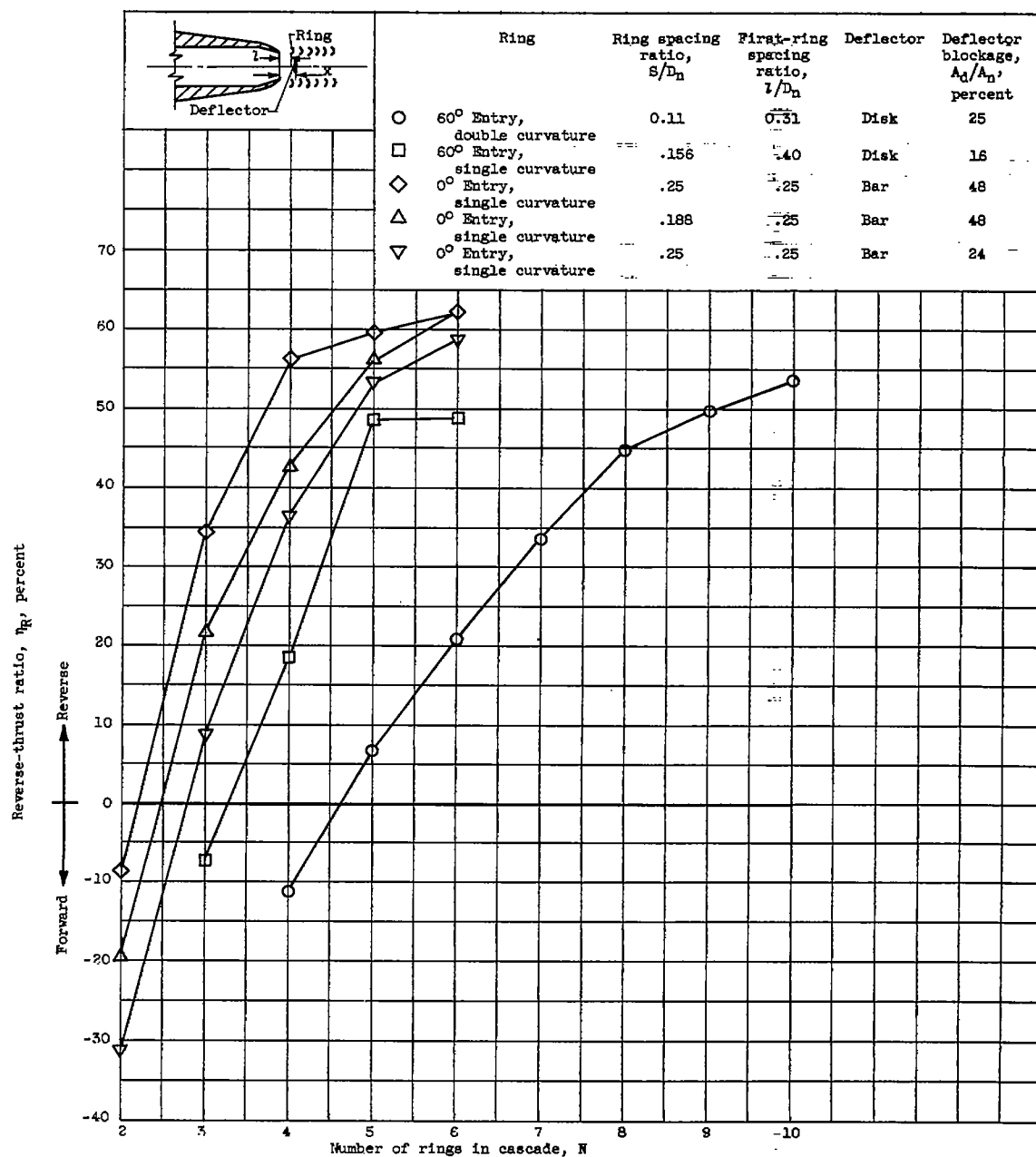


Figure 17. - Effect of number of rings on reverse-thrust ratio. Air flow ratio, 100 percent; exhaust-nozzle pressure ratio, 2.0.

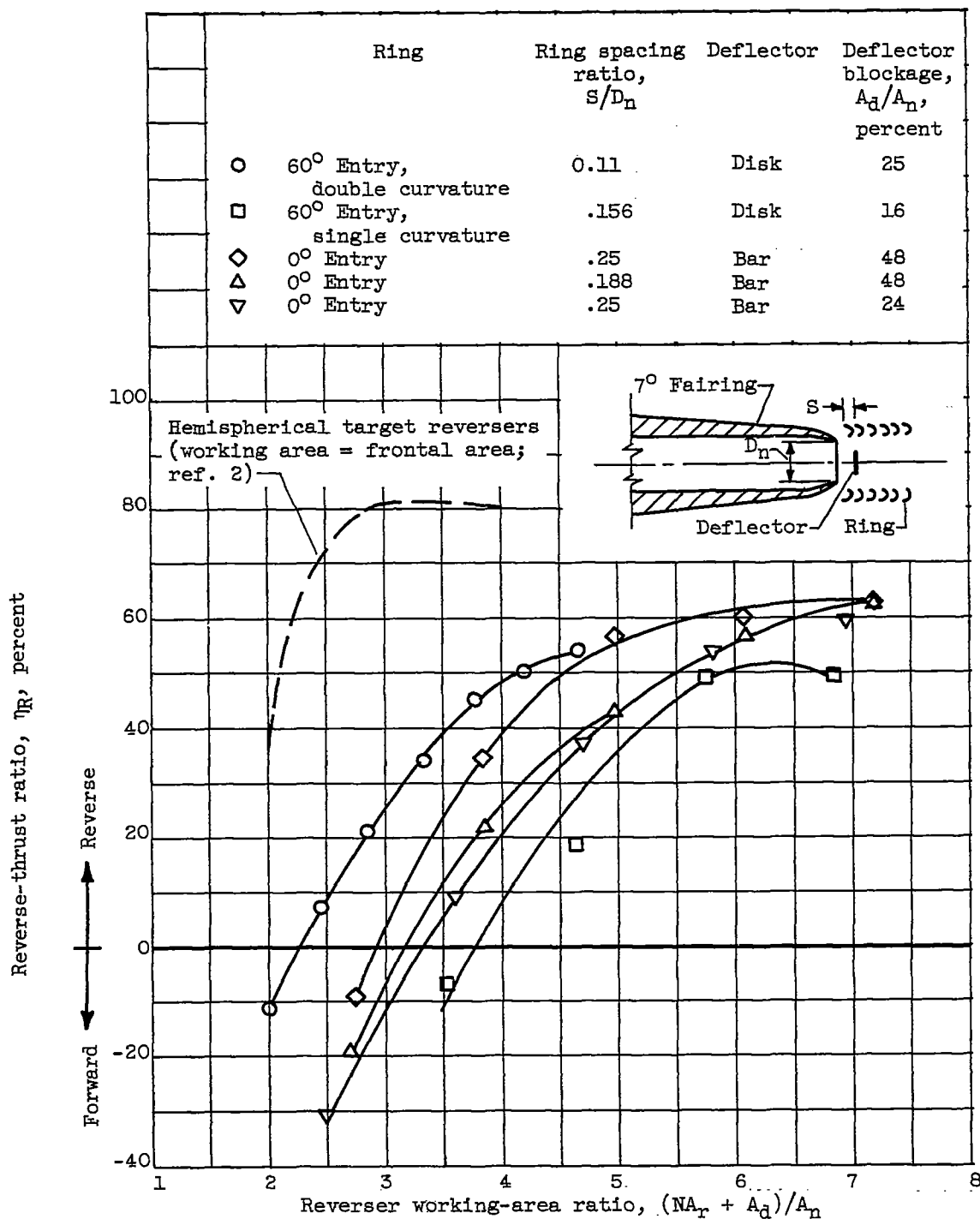


Figure 18. - Effect of reverser working-area ratio on reverse-thrust ratio. Air flow ratio, 100 percent; exhaust-nozzle pressure ratio, 2.0.

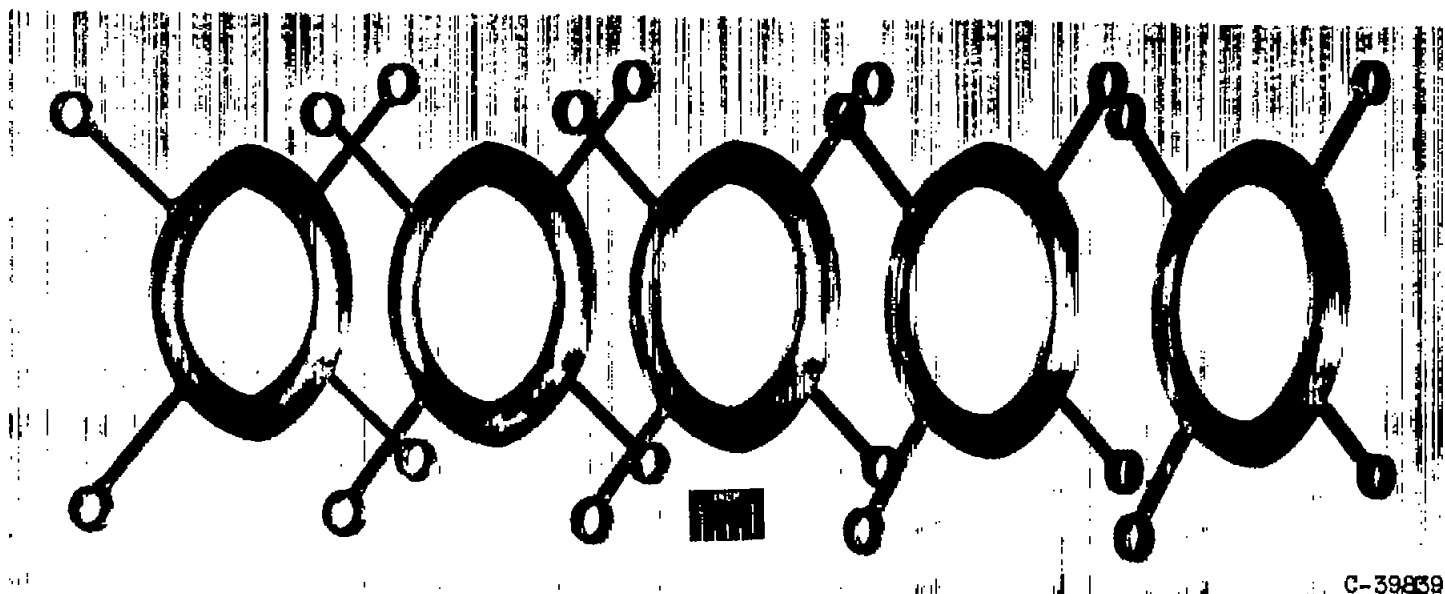


Figure 19. - Exploded three-quarter view of "split" cascade.

C-39839

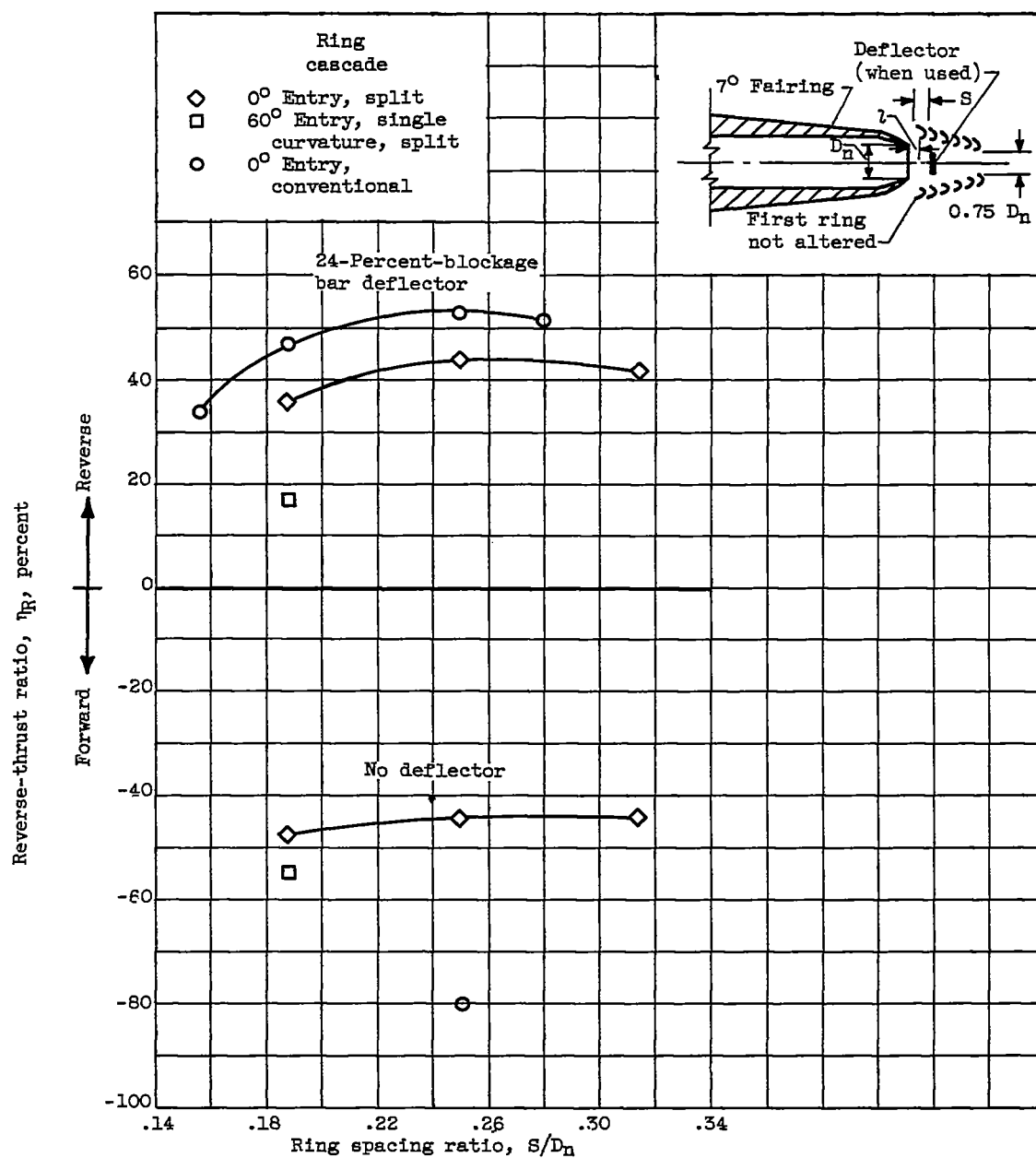
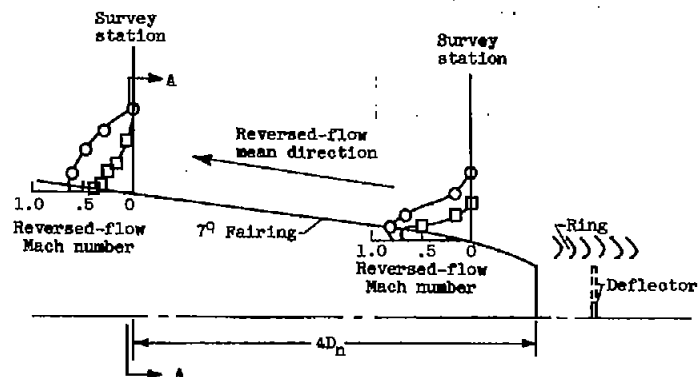
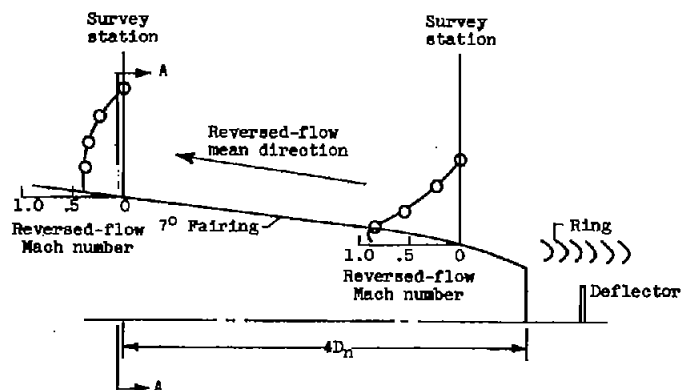
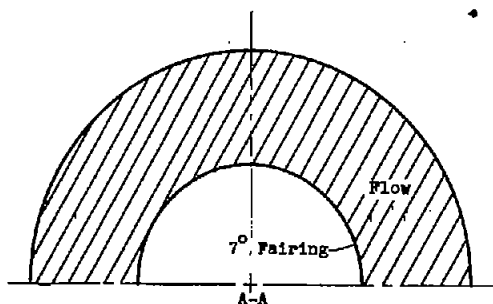


Figure 20. - Performance of split-cascade thrust reversers. Six rings; first-ring spacing ratio, about 0.35; air flow ratio, 100 percent; exhaust-nozzle pressure ratio, 2.0.

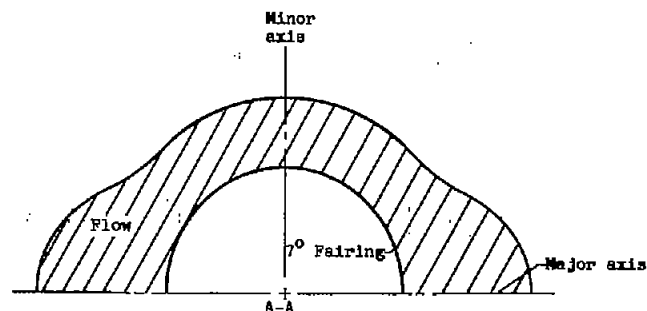
○ Top view (horizontal plane)  
 □ Side view (vertical plane)  
 Deflector mounted with long  
 edge vertical



Scale drawings

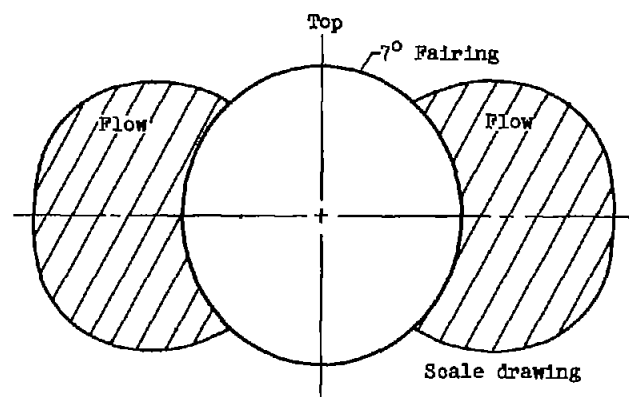


(a) 50-Percent-blockage flat-disk deflector; reverse-thrust ratio, 59 percent.



(b) 48-Percent-blockage flat-bar deflector; reverse-thrust ratio, 47 percent.

Figure 21. - Reversed-flow characteristics of typical unshrouded ring-cascade reversers. Six 60°-entry single-curvature rings; air flow ratio, 100 percent; exhaust-nozzle pressure ratio, 2.0.



(a) Typical reversed-flow field at station 4 nozzle diameters forward of exhaust nozzle for  $\alpha_0 = 85^\circ$  shrouds over top and bottom of cascade. 48-Percent-blockage bar deflector with long side vertical; reverse-thrust ratio, 28 percent.

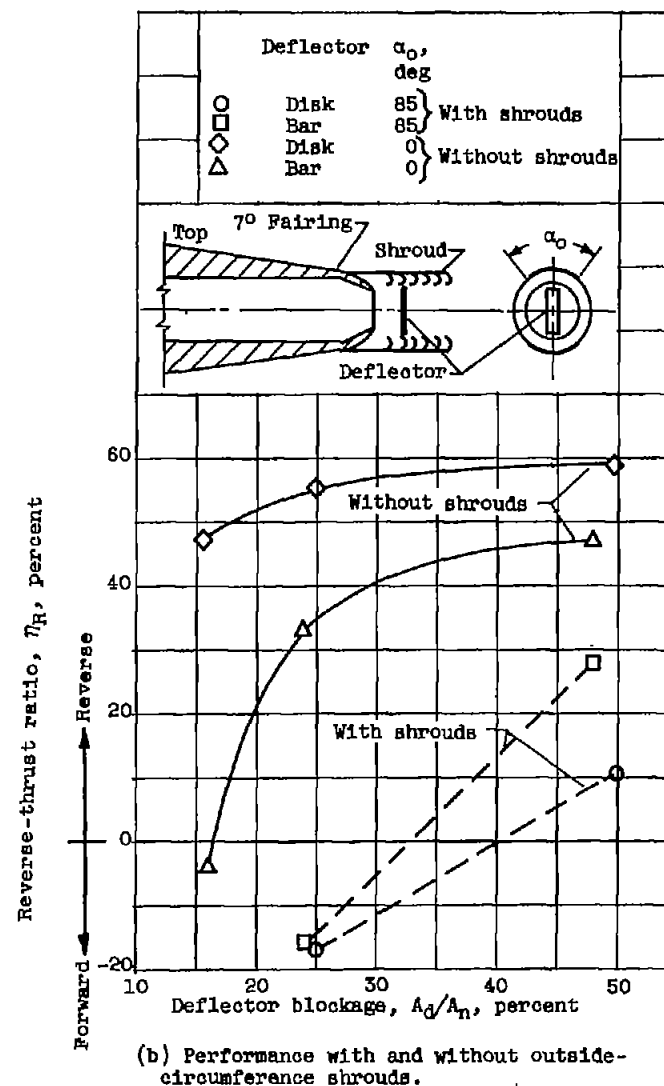
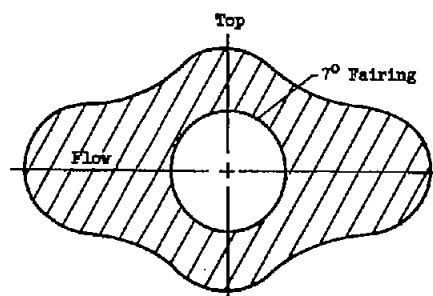
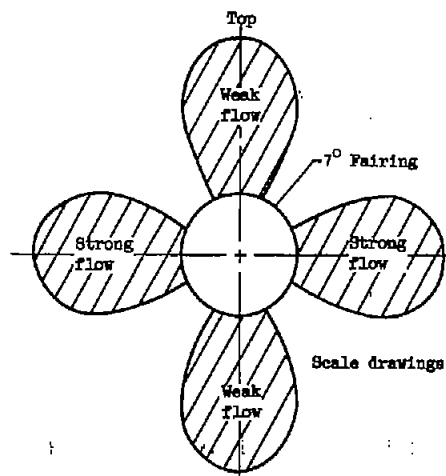


Figure 22. - Performance and reversed-flow field of ring-cascade reverser with shrouds over outside circumference of cascade. Six  $60^\circ$ -entry single-curvature rings; ring spacing ratio, 0.156; first-ring spacing ratio, 0.40; air flow ratio, 100 percent; exhaust-nozzle pressure ratio, 2.0.





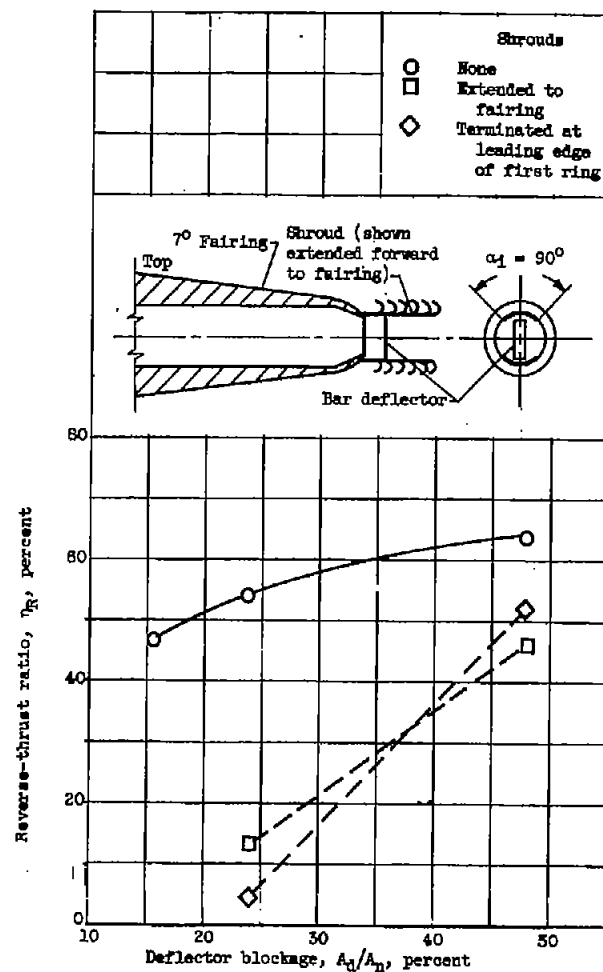
Shrouds terminated at leading edge of first ring; reverse-thrust ratio, 52 percent



Shrouds extended to fairing; reverse-thrust ratio, 46 percent

(a) Reversed-flow fields at station 4 nozzle diameters forward of exhaust nozzle. 48-Percent-blockage deflector.

Figure 25. - Performance and reversed-flow fields of reversers with inside-circumference shrouds,  $\alpha_1 = 90^\circ$ . Six  $0^\circ$ -entry rings; ring spacing ratio, 0.25; first-ring spacing ratio, 0.31; air flow ratio, 100 percent; exhaust-nozzle pressure ratio, 2.0.



(b) Performance with and without shrouds.

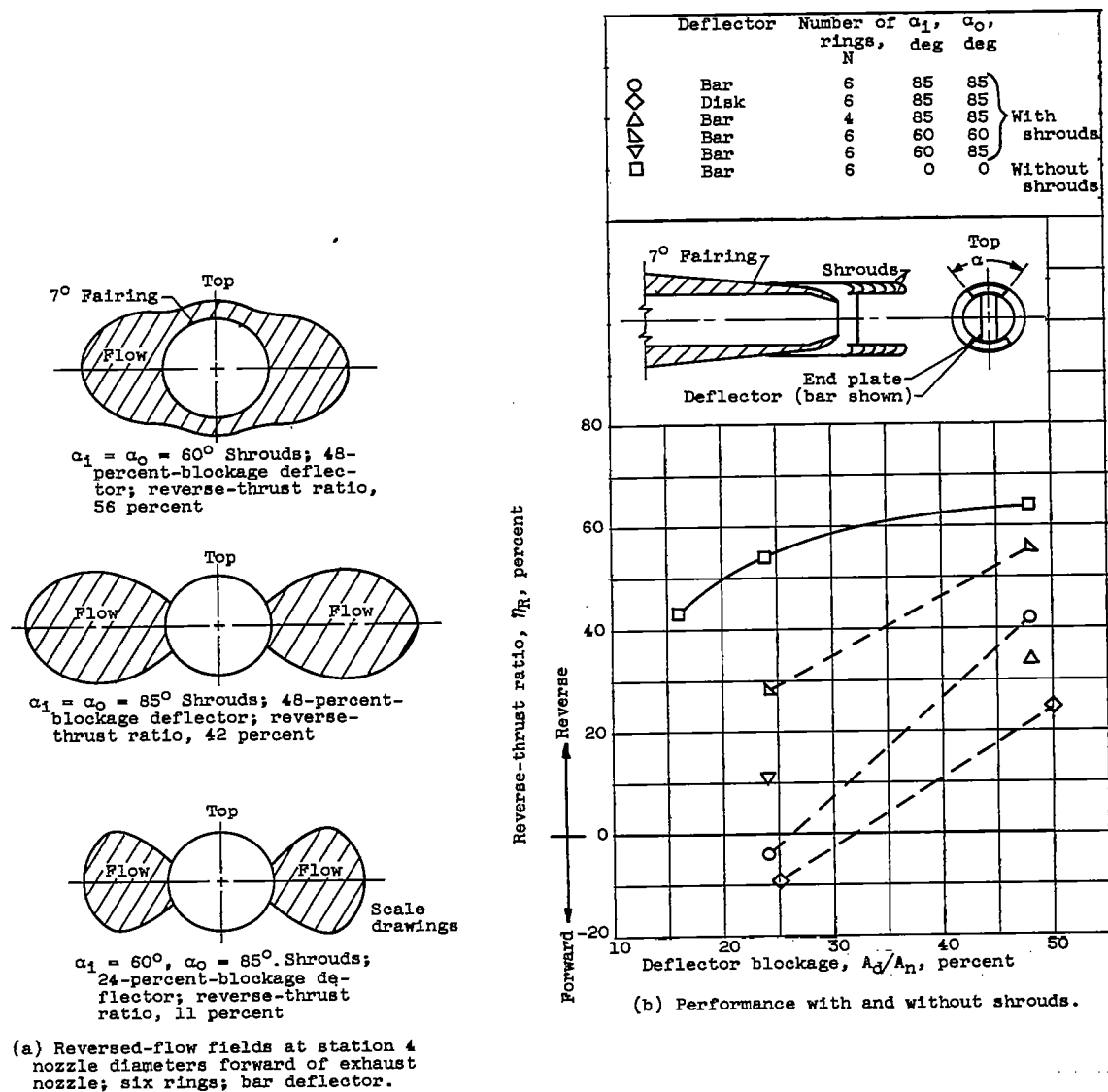
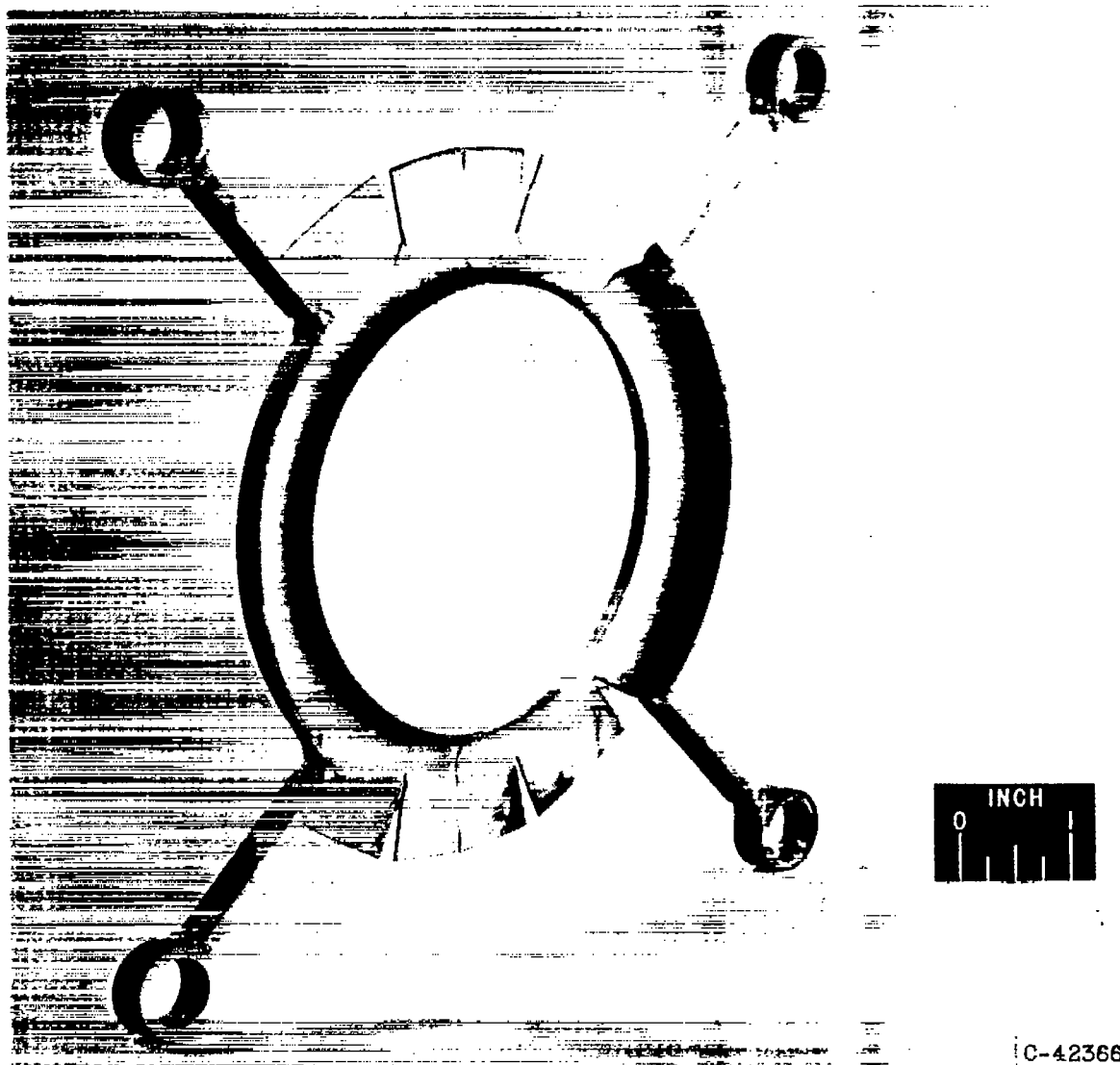


Figure 24. - Performance and reversed-flow fields of ring-cascade reversers with shrouds on both inside and outside circumference of cascade. ○-Entry rings; ring spacing ratio, 0.25; first-ring spacing ratio, 0.31; air flow ratio, 100 percent; exhaust-nozzle pressure ratio, 2.0.



C-42366

Figure 25. - Three-quarter view of O<sub>2</sub>-entry ring modified by bending two opposite 85° sectors to discharge gas in radial direction,

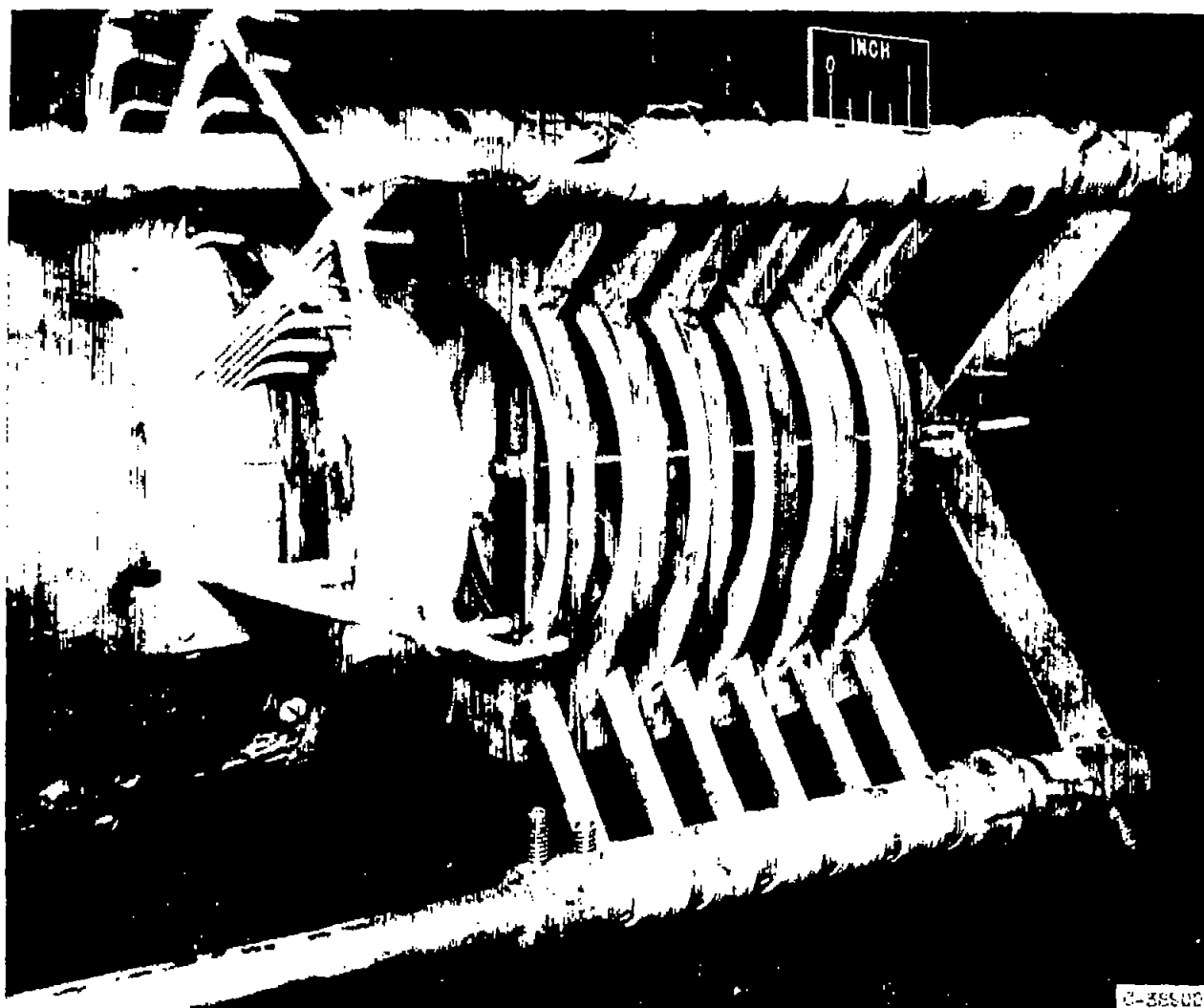
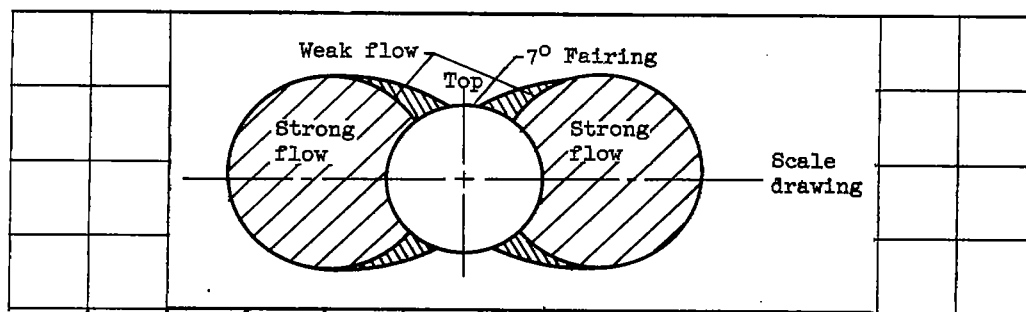
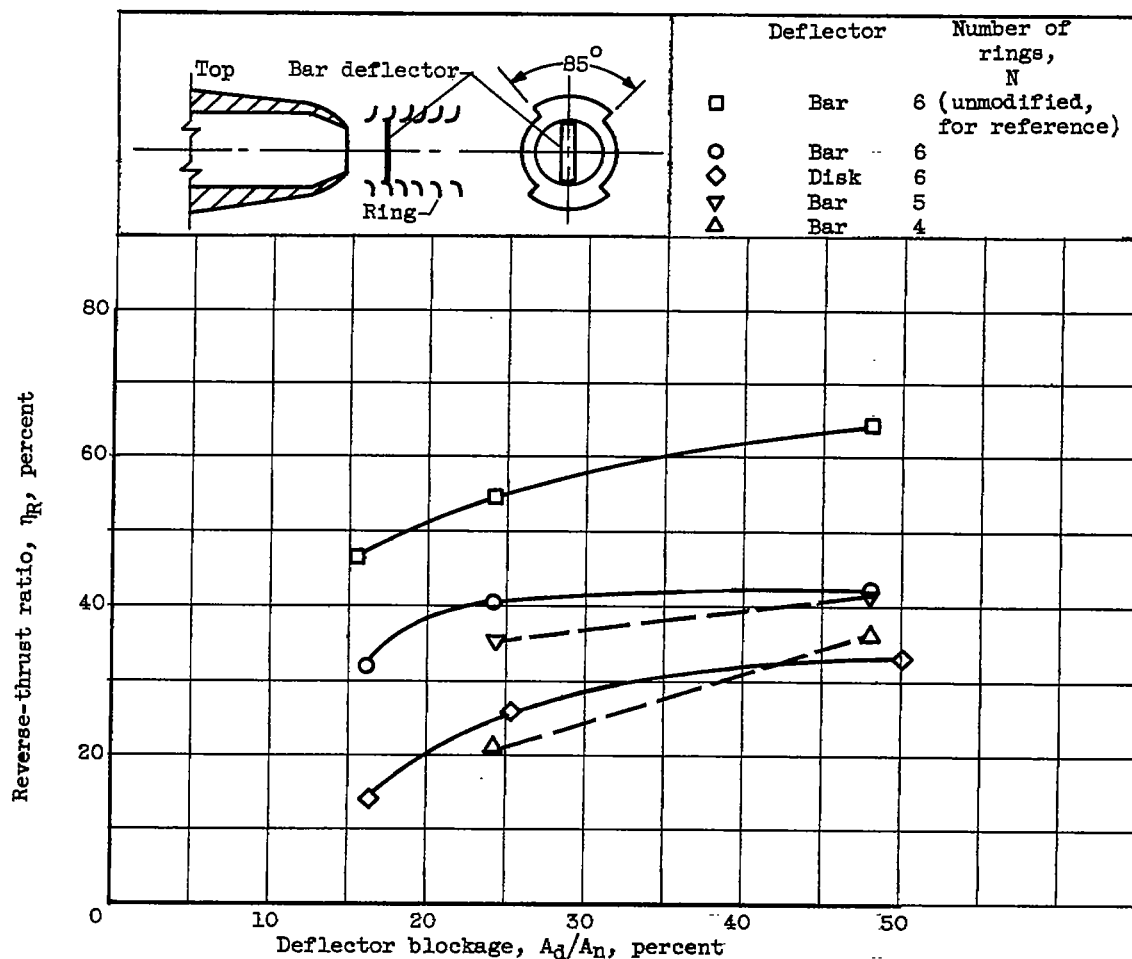


Figure 26. - Three-quarter view of reverser with six modified 0°-entry rings (fig. 25).



(a) Reversed-flow field at station 4 nozzle diameters forward of nozzle.



(b) Performance with and without modification.

Figure 27. - Performance and reversed-flow field of ring-cascade reverser in which two  $85^\circ$  sectors of cascade are modified to discharge gas in radial direction.  $0^\circ$ -Entry rings; ring spacing ratio, 0.25; first-ring spacing ratio, 0.31; air flow ratio, 100 percent; exhaust-nozzle pressure ratio, 2.0.

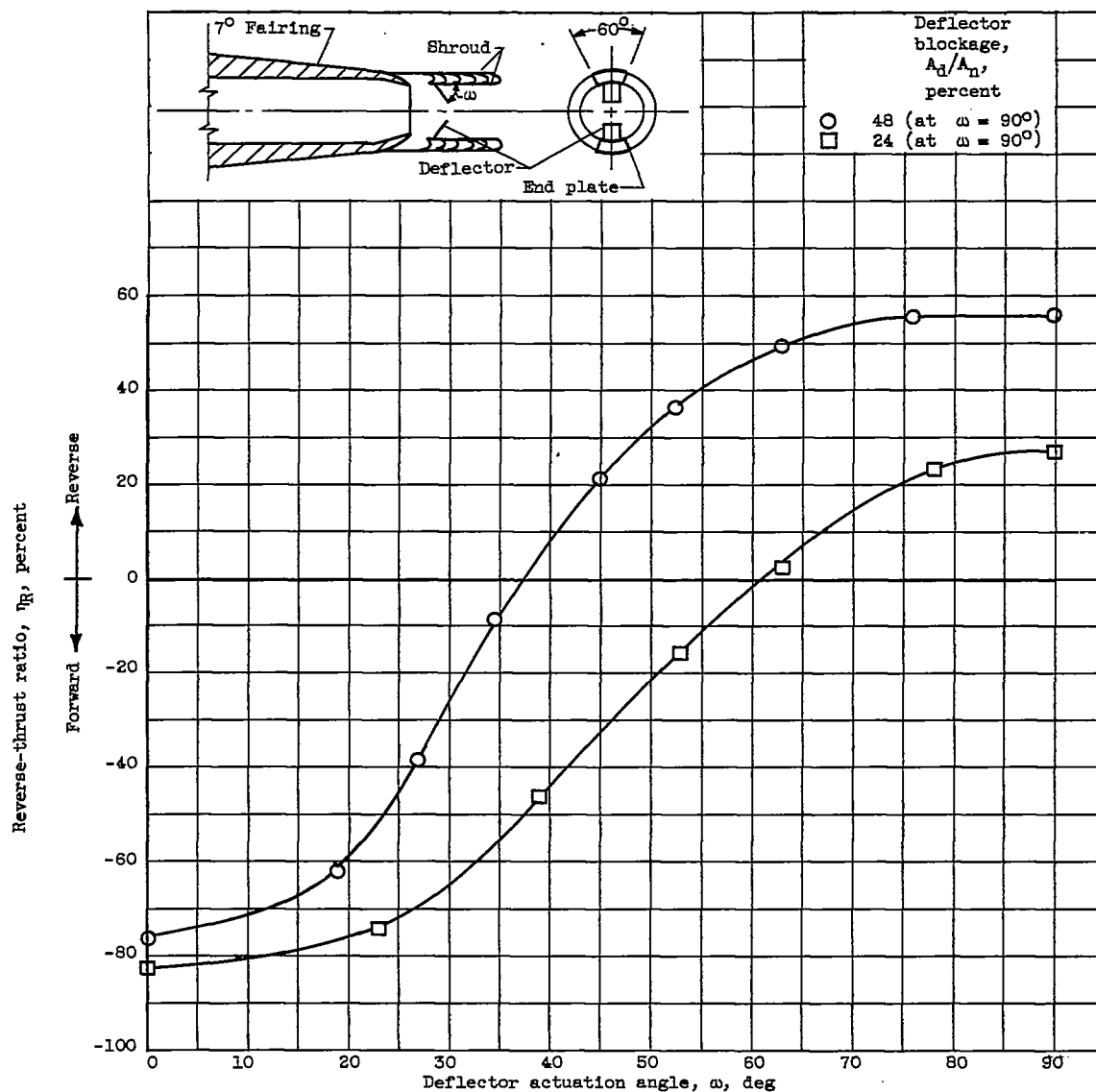


Figure 28. - Thrust modulation for ring-cascade thrust reverser. Six 0°-entry rings; ring spacing ratio, 0.25; first-ring spacing ratio, 0.31;  $\alpha_1 = \alpha_0 = 60^\circ$  shrouds; bar deflector; air flow ratio, 100 percent; exhaust-nozzle pressure ratio, 2.0.